arXiv:2503.04852v3 [cs.CV] 29 Oct 2025

CAUSAL3D: A COMPREHENSIVE BENCHMARK FOR CAUSAL LEARNING FROM VISUAL DATA

Disheng Liu[1]*, **Yiran Qiao**[1]*, **Wuche Liu**[1], **Yiren Lu**[1], **Yunlai Zhou**[1], **Tuo Liang**[1], **Yu Yin**[1], **Jing Ma**[1]
[1]Case Western Reserve University
{disheng.liu, yiran.qiao, wuche.liu, yiren.lu, yunlai.zhou, tuo.liang,yu.yin, jing.ma5}@case.edu

ABSTRACT

True intelligence hinges on the ability to uncover and leverage hidden causal relations. Despite significant progress in AI and computer vision (CV), there remains a lack of benchmarks for assessing models' abilities to infer latent causality from complex visual data. In this paper, we introduce **CAUSAL3D**, a novel and comprehensive benchmark that integrates structured data (tables) with corresponding visual representations (images) to evaluate causal reasoning. Designed within a systematic framework, Causal3D comprises 19 3D-scene datasets capturing diverse causal relations, views, and backgrounds, enabling evaluations across scenes of varying complexity. We assess multiple state-of-the-art methods, including classical causal discovery, causal representation learning, and large/vision-language models (LLMs/VLMs). Our experiments show that as causal structures grow more complex without prior knowledge, performance declines significantly, highlighting the challenges even advanced methods face in complex causal scenarios. Causal3D serves as a vital resource for advancing causal reasoning in CV and fostering trustworthy AI in critical domains. Datasets link https://huggingface.co/datasets/LLDDSS/Causal3D_Dataset

1 INTRODUCTION

Computer vision (CV) has achieved remarkable success in tasks such as classification (Dosovitskiy et al., 2021; Singh et al., 2022; Fang et al., 2023) and detection (Liu et al., 2021; Wang et al., 2023). Although these systems excel at identifying statistical correlations within data, they often struggle to infer deeper causal relations. This limitation significantly impacts their ability to be applied to high-stakes domains or unseen scenes. For instance, without understanding the causal relations between object depths, motions, and shapes, a vision-based autonomous driving system may easily misidentify traffic signs due to spurious correlations or adversarial attacks, leading to sudden braking and severe safety issues (Yang et al., 2022).

Unlike classification and detection tasks, which have thrived on large-scale datasets with explicit labels, causal tasks in images demand more for study and evaluation — ideally, annotations with clear causal relations among variables. This makes dataset collection significantly more challenging than in traditional CV tasks. The difficulty stems from two key factors: **inherent complexity and covert nature of causality**: Real-world causal relations are often complex and not directly observable, and causal variables are often high-level concepts (e.g., an object) instead of low-level pixels, making causal relations in vision domain inherently challenging to discern; **challenges in visual representation**: Even well-established causal rules are challenging to visually depict. For example, in physics, magnetic fields are represented by invisible magnetic induction lines, making them difficult to illustrate in realistic images. Similarly, abstract concepts like economic principles, (e.g., supply and demand), are not easily encoded into visual forms.

Some existing datasets have been involved in causal studies in visual AI systems. However, these datasets often have significant limitations. For instance, oversimplified 2D hypothetical

* These authors contribute equally.

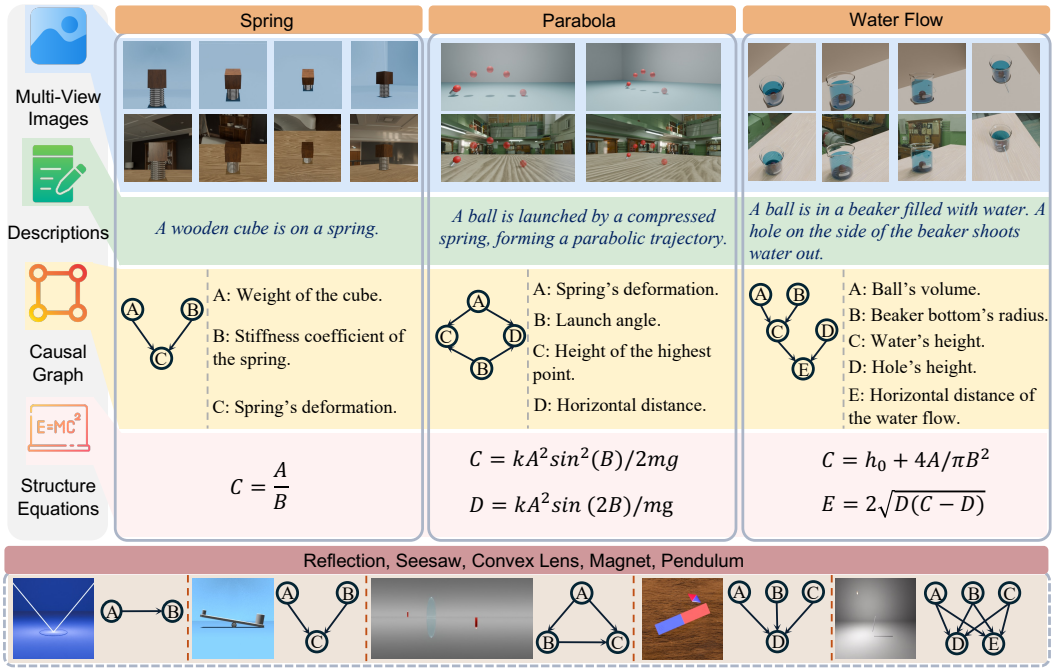


Figure 1: The proposed CAUSAL3D dataset. We display 8 real-world scenes (11 hypothetical scenes are in the Appendix 6). We focus on 3 scenes: springs, parabolas, and water flow. 1) The blue block represents multi-view images of each scene, offering four different views. The first row shows virtual backgrounds, while the second row shows real backgrounds, with the same view in each column; 2) The green block provides textual descriptions; 3) The yellow block represents the causal graphs for each scene, along with the meanings of each variable in the graphs; 4) The pink block shows the structural equations (i.e., functions describing causal relations) for each scene. The bottom row briefly presents an overview of the remaining 5 real-world scenes and their corresponding causal graphs, including reflection, seesaw, convex lens, magnet, and pendulum. Detailed information on these 5 scenes can be found in the Appendix 6.

datasets (Yang et al., 2020) fail to capture the richness and complexity of real-world environments. Similarly, domain-specific datasets like the CelebA face dataset (Liu et al., 2015) are not designed for causal reasoning and lack the structural diversity required for comprehensive explorations. Recent datasets developed for vision- and multimodal-language models (VLMs/MLMs) (Zimmermann et al., 2021; Von Kügelgen et al., 2021; Mao et al., 2022; Tung et al., 2024) have improved in complexity and realism but remain limited in explicitly representing causality and in offering diverse causal relations. The absence of clearly defined causal relations within visual representations, along with the lack of tabular records that are tightly aligned with these representations to provide guidance, makes such physics-aware VLMs/MLMs datasets suboptimal for fine-grained causal reasoning tasks. Especially, as interest in 3D data grows, causal learning in 3D settings introduces new challenges, opportunities, and insights. The complexity of realistic 3D scenes—encompassing lighting, texture, background, and viewpoint—can introduce spurious correlations and backdoor paths, making causal inference more difficult. At the same time, 3D environments provide multi-view consistency, allowing models to observe the same underlying causal relationships from diverse perspectives, which helps disentangle true causality from viewpoint-dependent features. This makes **3D datasets uniquely valuable for developing and evaluating robust, causally grounded models in realistic settings**. However, this area remains underexplored.

In general, existing visual datasets either lack explicit definitions of causal relations beyond visual representation or are too specific and simplified to enable comprehensive exploration of diverse causal relations. On the other hand, datasets in the causal research community, while rich in diverse causalities and clear causal definitions, lack corresponding visual representations, making them unsuitable for tasks involving causal reasoning in images, not to mention complicated 3D scenarios. This disconnect makes it challenging to effectively advance and evaluate AI systems' abilities of reliable reasoning, thereby creating a significant bottleneck in advancing this field.

Table 1: Qualitative comparison between Causal3D and other causality related dataset. "Diverse Structure" refers to whether the dataset covers different causal graph structures, e.g., our dataset involves 13 different graph structures spanning from real and hypothetical scenes.

Dataset	Dual Representation of Causality		Explicit Causal Structures		Hybrid Causal Framework		Diverse Structure and 3D Scenes	
	Tabular	Visual	Linear	Nonlinear	Physical Consistent	Hypothetical Scenes	Diverse Structure	Diverse 3D Scenes
CauseMe (Runge et al., 2019a)	✓	✗	✓	✓	✗	✓	✗	✗
CelebA (Liu et al., 2015)	✓	✓	✗	✗	✗	✓	✗	✗
CausalVAE (Yang et al., 2020)	✓	✗	✓	✓	✓	✓	✗	✗
Causal3DIdent (Zimmermann et al., 2021)	✗	✓	✓	✗	✓	✗	✗	✓
Craft (Ates et al., 2022)	✗	✗	✓	✗	✓	✗	✗	✗
CLEVR-Humans (Mao et al., 2022)	✗	✓	✓	✗	✓	✗	✗	✓
Physion++ (Tung et al., 2024)	✗	✓	✓	✓	✓	✗	✗	✓
Causal3D	✓	✓	✓	✓	✓	✓	✓	✓

To address these limitations, we introduce **CAUSAL3D**, the first benchmark specifically designed to systematically explore and evaluate causality learning through a combination of realistic 3D imagery and explicit causal structures (*i.e.,* causal graphs and structure equations). Using CAUSAL3D, we conduct experiments on existing algorithms and tools, **establishing a comprehensive benchmark** to evaluate models' abilities to identify and leverage diverse causal relations.

To the best of our knowledge, CAUSAL3D (see Fig. 1) is the first dataset tailored for causality studies that combines realistic 3D scenes with explicit causal graphs (i.e., Directed Acyclic Graphs (DAGs) representing variables as nodes and causal relations as edges). This dataset stands out due to several key features: **1) Dual Representation of Causality**: CAUSAL3D provides a dual representation of causality by including both tabular data (for high-level concepts) and strongly corresponding visual representations in multiple 3D scenes. This design provides sufficient information for causal studies in vision, enabling precise evaluations of models in related domains. **2) Diverse Design**: The difficulty in CAUSAL3D is diversely structured, derived from different dimensions, including the number of variables (ranging from 2 to 5), multiple causal structures, different (linear/nonlinear) types of causal relations, and various camera views and backgrounds in 3D scenes. This design enables benchmarking with progressively increasing levels of challenges, allowing for fine-grained evaluation of model performance. **3) Physically Consistent and Hypothetical Scenes**: CAUSAL3D encompasses both real-world and hypothetical scenes. By leveraging established physical rules, it creates datasets with realistic causal relations, enhancing the dataset's authenticity. To further diversify causal scenes, CAUSAL3D incorporates hypothetical causal relations, providing a broader range of possibilities and enriching its utility for causality research. With the dataset, we designed systematic experiments to evaluate representative causal methods and LLMs/VLMs in different causal tasks. In this work, our primary contributions are threefold:

- **Dataset** We introduce CAUSAL3D, a novel and comprehensive benchmark consisting of 19 datasets that span a wide range of causal structures, viewpoints, and background variations within realistic 3D scenes. The full dataset will be released to support further research.
- **Evaluation** We implement a thorough evaluation of models on CAUSAL3D, spanning from traditional causal algorithms to advanced LLMs and VLMs for images, offering a detailed analysis of the current state-of-the-art models on our benchmark.
- **Insights** We lay a strong foundation for advancing causal learning in CV by bridging the gap between these fields through our benchmark and provide key insights from our experimental observations.

2 RELATED WORK

Causal Discovery from Tabular Data Causal discovery is an important task in causal inference (Pearl, 2009), aiming to identify the causal relations from data. Multiple methods have been developed for this task and most of them focus on tabular data (Wen et al., 2021; Tu et al., 2024; Wen et al., 2022; Cinquini et al., 2021; Russo and Toni, 2023). These methods mainly include constraint-based methods (e.g., PC (Spirtes et al., 2000b)) and score-based methods (e.g., GES (Chickering, 2002)). Many of them are statistical methods (e.g., CAM (Bühlmann et al., 2014), LiNGAM (Yang et al., 2024)), which have good theoretical support but often suffer from strong assumptions, sensitivity, and scalability issues.

Recently, deep learning-based methods have attracted lots of attention due to their improvement in these aspects. Among them, causal-TGAN (Wen et al., 2022), GraN-DAG (Lachapelle et al., 2020), DAG-GNN (Yu et al., 2019)) can model nonlinear causal relations in large datasets. Diffusion-based approaches (e.g., DiffAN (Sanchez et al., 2023)) improve robustness against noises while being computationally intensive and sensitive to hyperparameters.

LLM-based Causal Discovery Recent advances in LLMs have broadened their role in causal discovery (Ma, 2024; Jin et al., 2024; Liu et al., 2024b; Ban et al., 2023; Liu et al., 2024a; Wu et al., 2024; Wan et al., 2024; Shen et al., 2024). LLM-based causal discovery spans pairwise and full-graph discovery (Ma, 2024; Kıcıman et al., 2023; Jiralerspong et al., 2024), often leveraging prompts such as binary or multiple-choice selection and natural question-answering. Among them, many state-of-the-art models like ChatGPT 4o (Rawal et al., 2024) and Gemini-1.5 Pro (Carro et al., 2024) have been widely explored for causal inference. Besides, some causality-specific agents like Causal Copilot (Wang et al., 2024b) integrate LLMs for natural language-based causal queries. Despite its promising performance, LLMs still face key limitations, including difficulty in handling latent confounders and complex causal tasks.

Causal Methods in CV Causal inference in CV is essential for improving generalization and interpretability (Yang et al., 2021; Schölkopf, 2022). Many causal tasks have thus been widely explored in image data, one of them is causal representation learning, which aims to uncover disentangled and causally meaningful representations corresponding to high-level variables from data (Liu et al., 2022; Deng et al., 2022; Schölkopf et al., 2021). Many representative approaches in this area are based on generative models (e.g., CausalVAE (Yang et al., 2023), DEAR (Shen et al., 2022)). However, they often depend on strong assumptions (e.g., available annotation of high-level concepts) that may not always hold. Recently, explorations of VLMs in causal tasks under more general scenes have also attracted increasing attention (Wang et al., 2024a; Zhao et al., 2024).

Causal Datasets in CV Tabular data has long dominated causal inference research (Runge et al., 2019a; Runge, 2018; Runge et al., 2019b; Spirtes et al., 2000a; Zheng et al., 2018). With the recent increasing need for causal studies in different data types and modalities, the community in CV and VLM has also placed more emphasis on causality. Recent years have witnessed the emergence of image and video datasets for causal reasoning (Zimmermann et al., 2021; Ates et al., 2022; Mao et al., 2022; Tung et al., 2024), bridging the gap between CV learning and causal reasoning. Despite these datasets addressing the absence of visual data encoded with causality, most of them still remain limited. They either focus on specific scenes, restricting the diversity of causal relations or lack rigorous causal definitions—such as explicit causal graphs and structured tabular records—to capture interactions among in-image variables. Consequently, a gap remains between traditional causal research and the study of causality in CV and VLM, as summarized in Tab. 1. This highlights the need for datasets that integrate explicit causal structures with both visual and tabular representations.

3 CAUSAL3D: THE PROPOSED BENCHMARK

We introduce CAUSAL3D, a realistic 3D image dataset designed for casual learning from *observational* visual data. Aiming to bridge the gap between causal study and CV/VLM community, CAUSAL3D is established with structured tabular data and tightly aligned visual representation. To build a comprehensive benchmark for evaluating models' ability to uncover causality, CAUSAL3D contains visual representations encoded with diverse causal relations among multiple variables. The dataset comprises two main components: **Physically Consistent 3D Scenes**, which simulate real-world settings to enhance the authenticity of the dataset, and **Hypothetical 3D Scenes**, introduced to diversify the causal relations represented in the dataset. To simulate realistic images in 3D scenes, we select or design causal relations to generate structured datasets and use Blender[1] to render high-quality images, as shown in Fig. 2. Furthermore, by introducing various views and backgrounds, CAUSAL3D presents the same scene in different surroundings, enhancing dataset diversity and contextual richness.

3.1 DATASET COMPONENTS

Physically Consistent Scenes In the physically consistent setting, CAUSAL3D incorporates fundamental physical principles, such as light dynamics, magnetic fields, water pressure, and mechan-

[1] https://www.blender.org/

ics, to ensure realistic causal relations. To systematically vary the complexity of causal discovery, we curated 8 distinct scenes, each featuring 2 to 5 variables with unique causal structures. Each scene contains 10K samples. We provide vis

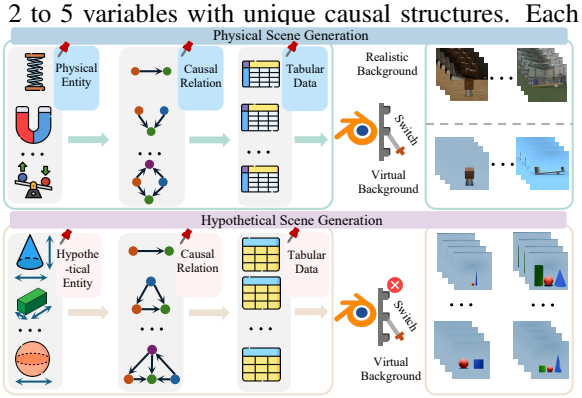


Figure 2: Illustration of data construction pipeline.

Hypothetical Scenes Since causal relations in reality are often complex and difficult to observe, designing scenes with diverse causal graphs is challenging. In CAUSAL3D, we also introduce additional hypothetical scenes that broaden the range of causal relations in our benchmark. Specifically, we explore causal relations under artificially defined hypothetical rules and synthesize causal relations among three fundamental 3D objects in Blender: sphere, cuboid, and cone. By defining specific dependencies among their variables (*e.g.,* sphere radius, cuboid height), we construct both linear and non-linear causal relations across various graph configurations. This process yields 11 hypothetical scenes, each containing 10K samples. More details can be found in Appendix 6.

3.2 DATA CONSTRUCTION

The data construction process is shown in Fig. 2. The upper half shows the construction of real physical scenes. We first collect physical entities that exist in the real world, such as springs and magnets, etc. Then, we explore the physical laws within these entities and identify the corresponding causal graphs. Based on the causal graphs, we can generate tabular data, where each row represents a sample, and different columns correspond to different values of various variables. For variables without parents, we assign values randomly using a uniform distribution, while the values of other variables are calculated according to the causal graphs and physical laws. For example, if we select a spring and a block as our physical entities, the variables involved include the spring constant k, the deformation X, and the weight of the block W. The physical law governing these variables is Hooke's Law: $X = W/k$. We can randomly assign values to W and k, and then calculate X accordingly. The generated tabular data can then be input into Blender to render multi-perspective scenes. It is worth noting that we have set a background switch to choose whether to use a real or virtual background. The lower half of Fig. 2 displays the construction of hypothetical scenes. We first identify various dimensions of geometric bodies to serve as variables and then manually design the relations among these variables. The remaining steps are the same as those in generating physical scenes, with the only difference being that they do not include real backgrounds because the hypothetical objects and relations do not exist in the real world.

3.3 TASK DESIGNS

Based on our dataset, we focus on three key causal tasks to evaluate state-of-the-art algorithms and models in discovering and leveraging causal relations across diverse causal structures and scenes. We focus on the widely adopted setting of causal learning from observational data. These tasks include:

Causal discovery from tabular data This task focuses on identifying latent causal relations among variables using only tabular data. In this setting, we have high-level causal variable values recorded in the tabular data and do not rely on image information. It is evaluated based on the correctness of inferred causal structures across various datasets and underlying causal mechanisms.

Causal representation learning from images This task aims to learn disentangled and causally meaningful representations from images, meanwhile enabling models to capture underlying causal relations between high-level concepts. We use image data along with any additional information required by the models as input. Evaluation is based on generated images after intervening on learned representations, assessing whether they accurately reflect the corresponding causal variables and causal relations.

Causal discovery & intervention from few images This task focuses on uncovering causal relations and assessing intervention results with a limited number of images. Unlike traditional causal

discovery methods that rely on large datasets, this task evaluates the ability of models to infer causal structures from a small set of images. Furthermore, we conduct causal interventions by manipulating a certain variable to observe its effect on the whole image. Causal intervention is often implemented with the do-operator $do(\cdot)$ (Pearl, 2009). Here, $do(X = x)$ means modifying a variable X to a specific value x while keeping all other influences unchanged. Intervention evaluation is based on whether the intervened images still remain consistent with the underlying causal relations.

4 EVALUATIONS

Overview. In this section, we conduct a systematic evaluation on our benchmark Causal3D, focusing on three major causal tasks as aforementioned. For each task, we select appropriate models to assess their performance across diverse scenes. For causal discovery from tabular data, we evaluate traditional causal discovery methods alongside an LLM-based causal agent. For causal representation learning, we benchmark state-of-the-art methods to examine their ability to extract meaningful causal factors. Lastly, for causal discovery and intervention from few images, we test various VLMs with different prompts. Our experiments span multiple settings with comprehensive insights.

4.1 EXPERIMENT SETTINGS

Data Preprocessing. Both image and tabular data were meticulously prepared to ensure seamless compatibility with the evaluated models. Image data were resized and normalized as required, and tabular data were formatted to meet the input specifications of traditional causal discovery methods.

Evaluation Metrics. We mainly use two metrics to quantify the experimental results: **1) F1 Score** is used to evaluate causal discovery results, which represents the harmonic mean of precision and recall of discovered causal relations. **2) Accuracy** is used in causal intervention, which measures the fraction of consistent causal relations in the intervened image. Each experiment is repeated 10 times per setting, and the final results are obtained by averaging these results for robust evaluation.

4.2 CAUSAL DISCOVERY FROM TABULAR DATA

Evaluated Methods. We evaluate the performance of various causal discovery methods on tabular data, covering both traditional algorithms and emerging LLM-powered approaches. We assess 7 traditional methods: CAM, NoTears, DAG GNN, DiffAN, PC, SCORE (Rolland et al., 2022), and GraN DAG; 1 LLM-based method: Causal Copilot (Wang et al., 2024b). All experiments were conducted on an NVIDIA RTX 4090 GPU.

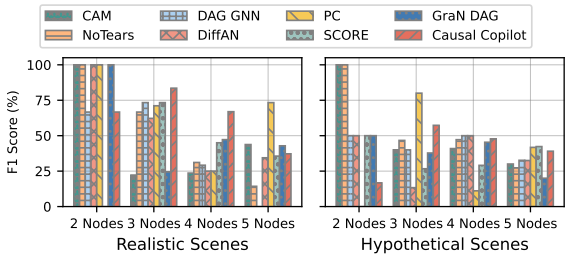


Figure 3: Results of different causal discovery methods from tabular data on realistic/hypothetical scenes.

Results and Analysis. The results are shown in Fig. 3. We test all methods on datasets representing both real and hypothetical scenes, categorized by causal graph complexity, ranging from 2- to 5-node structures. Each method takes the input of given tabular data and outputs a causal graph, and we compare it with the ground-truth causal graphs using the F1 score. The final evaluation metric is computed by averaging F1 scores within each node category. As shown in Fig. 3, although the performance of different methods varies within the same category, it can be observed in both realistic scenes and hypothetical scenes that there is a general downward trend in performance from 2-node to 5-node scenes. This aligns with our common sense and the laws of physics: the more variables there are in a scene, the more difficult it is to uncover the underlying rules.

4.3 CAUSAL REPRESENTATION LEARNING

Evaluated Methods. In this section, we evaluate causal representation learning models, including CausalVAE, DEAR, ICM-VAE (Komanduri et al., 2023), and CDG-VAE (An et al., 2023) on our dataset. The images and other information needed by models (e.g., CausalVAE requires annotations of causal variables) are taken as input. These methods are all based on the variational autoencoder

(VAE) framework and aim to learn a low-dimensional representation composed of multiple disentangled yet causally related latent variables inside images.

Evaluation Strategy. Since many of these models require a (partial) causal graph as input or supervision, it would be unfair to directly evaluate them with regular causal discovery metrics we used in the previous subsection. Following the evaluation strategy of previous works (Yang et al., 2020; Shen et al., 2022; Komanduri et al., 2023; An et al., 2023), we apply interventions on each variable separately by modifying its corresponding causal representations, and then decode the modified latent representation back to generate an intervened image. By assessing whether the causally related variables in the image change accordingly, we can evaluate whether the model has effectively learned the causal relations within our dataset.

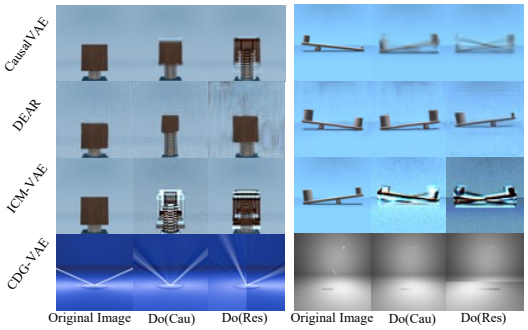


Figure 4: Examples of the 4 causal representation learning model results. In each scene, the 3 columns show: 1) original images, 2) Do(Cau): results after intervening on a "cause" variable, and 3) Do(Res): after intervening on a "result" variable.

Since these models only accept 2D images, we render the 3D scenes from a fixed viewpoint as inputs. For CausalVAE, DEAR, and ICM-VAE, we use ***spring*** and ***seesaw*** for evaluation. However, for CDG-VAE, which requires a structured mask to distinguish each object (i.e., variable), meaning that each object must move within a specific region, ***spring*** and ***seesaw*** do not satisfy this requirement. Therefore, we select ***reflection*** and ***pendulum*** for evaluation.

Results and Analysis. Intervention results are showcased in Fig. 4. For each given original image, we select a pair of "cause" and "result" variables to intervene with do-operation. For ***spring***, the cause is the weight of the wooden block, and the result is the spring's deformation. We first apply an intervention on the weight of the wooden block (cause), with the intervened image shown in the left-middle column. We observe that decreasing the block's weight leads to a corresponding decrease in the spring's deformation. This aligns with the causal relation, where the block's weight directly influences the spring's deformation. However, when we directly modify the spring's deformation (result), as shown in the left-last column, the block's weight remains unchanged. This confirms the unidirectional nature of causal relations, where the cause affects the effect, but not vice versa. The results for the ***seesaw*** scene exhibit a similar pattern. When we apply an intervention on the torque on the left side (cause), as shown in the right-middle column, the seesaw's direction (result) reverses accordingly. However, when we directly intervene on the seesaw's direction, the torque on both the left and right sides remains unchanged. Similar observations hold for ***reflection***, where the incident light serves as the cause and the reflected light as the result, and for ***pendulum***, where the pendulum's angle acts as the cause, influencing the position and length of its shadow.

Although these models may not perform optimally in certain scenes, exhibiting distortions in reconstructed images and incomplete disentanglement of attributes, they still capture some underlying causal relations. This indicates the rationality of our proposed benchmark and highlights the need for further research in achieving more effective causal representation learning from images.

4.4 Causal discovery from few images

Evaluated Methods. Unlike traditional causal discovery methods that rely on tabular data or large-scale training images, we leverage pretrained VLMs to perform causal discovery using a small number of images. In this section we use ChatGPT[2], Gemini[3] and Claude[4] to discover causal relations by few image examples and textual prompts in real and hypothetical scenes. The VLMs are tasked with uncovering causal relations by generating adjacency matrices representing causal graphs. Each prompt specifies key variables in the scenes, explicitly guiding the models to infer causal structures. We use 4 different prompting strategies, as detailed in Tab. 3 in the Appendix 7.

[2]https://platform.openai.com/docs/api-reference/introduction
[3]https://ai.google.dev/api?lang=python
[4]https://www.anthropic.com/api

1) Basic Prompts: General instructions that broadly guide the models to identify causal relations.

2) Explicit Function Prompts: The model is designated as a causal discovery expert to identify causal relationships among image variables.

3) Chain of Thought (CoT): The model is prompted to reason through the causal discovery process step by step without any prior examples. This approach encourages structured reasoning and provides insights into how the model interprets causal relations.

4) Few-Shot: The model is given three exemplar cases of causal discovery before performing the task, enabling it to generalize better by leveraging prior examples to improve causal relation identification. Performance is evaluated by comparing the generated adjacency matrices with the ground truth, providing a quantitative measure of the causal discovery task.

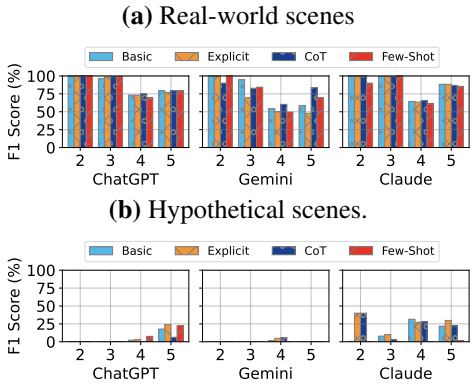


Figure 5: Causal discovery results of VLMs in various scenes, averaged over datasets with 2–5 nodes in the causal graph.

Results and Analysis. Demonstrated in Fig. 5(a), models performed significantly better in real-world scenes (e.g., governed by Hooke's Law, magnetic fields and etc.) compared to hypothetical scenes, benefiting from prior physical knowledge embedded in their LLM components. However, as causal relations became more complex and involved more variables, performance declined, highlighting the challenge of uncovering causality in such scenes. In the hypothetical scenes, the results, as shown in Fig. 5(b), reveal poor performance. This suggests that when prior real-world knowledge is unavailable and only a limited number of images are provided, models consistently fail to uncover latent causal relations. Consequently, current closed-source VLMs have been shown to be unreliable for causal discovery in hypothetical settings.

Views and Backgrounds. CAUSAL3D provides multi-view images of the same scene, simulating real-world 3D environments with both virtual and realistic backgrounds. This enables in-depth analysis of how different viewpoints and background contexts affect causal discovery performance. Case studies from the Spring and Parabola scenes are shown in Fig. 6. Within the experiments, different 3D views affect the performance in causal discovery. Interestingly, our results reveal that intuitive views, such as a front view, are not always the most effective for uncovering latent causality. Different viewpoints can either increase or decrease task difficulty, with no single "golden standard" view for causal discovery. Additionally, when comparing multi-view and single-view inputs in the causal discovery task, multi-view performance varies depending on the scene (as shown in Fig. 9). In scenes with simple causal relations (e.g., a spring system with a linear relation among three variables), multi-view inputs tend to degrade model performance, possibly introducing unnecessary noise. Conversely, in more complex 3D scenes with intricate causal dependencies, like a parabola scene involving nonlinear relations among four

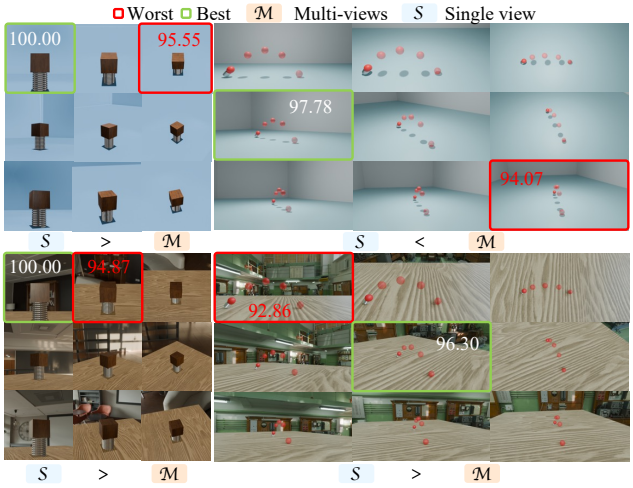


Figure 6: We select two scenes, **Spring** and **Parabola**. Using the F1 score as metric, we assess VLM performance in causal discovery. The best and worst views are highlighted to demonstrate the impact of different perspectives. To analyze the effect of multi-view vs. single-view images, we average the performance across 9 individual views in each scene and compare it with the overall multi-view performance. More detailed version is in Appendix 7.

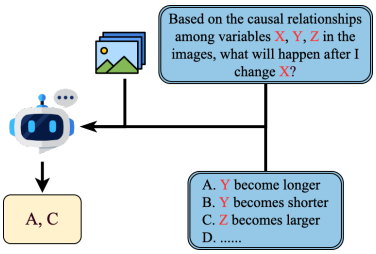


Figure 7: Example of intervention prompts for trained VLMs.

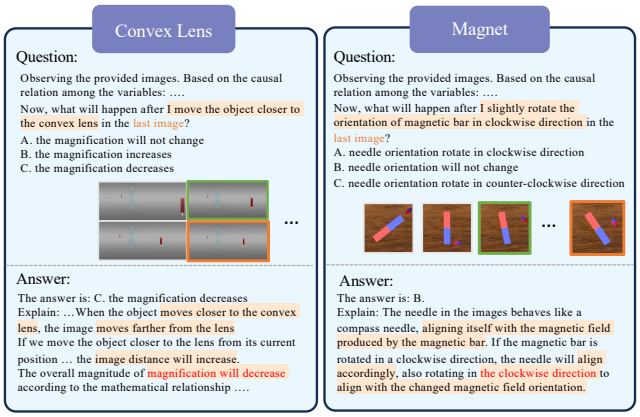


Figure 8: Case studies of failures. VLMs fail to grasp causality within physically consistent scenes for intervention tasks.

variables in the virtual background, multi-view perspectives enhance inference accuracy, suggesting that additional viewpoints help capture richer causal structures in such settings.

Comparing virtual and realistic backgrounds, we find that realistic backgrounds introduce additional noise, making causal discovery more challenging. Our experiments indicate that even when models leverage prior real-world knowledge encoded in LLMs, the presence of realistic background information increases task complexity and negatively impacts inference performance (quantitative results shown in Fig. 37 in Appendix 7).

4.5 Causal Intervention in VLMs

Evaluated Methods. To further assess the ability to learn causality from images, causal intervention serves as a crucial step beyond causal discovery. In this experiment, we leverage VLMs in interventions. This task is formulated as a multiple-choice problem, where the model must identify the correct outcomes based on induced causal changes. The detailed inference pipeline is illustrated in Fig. 7. In this setup, VLMs are provided with a few images along with questions about the variables present in the scene. By posing queries such as "*What will happen after changing variable X?*", we expect the model to return the correct answer based on the causal relations depicted in the given images. This evaluation determines whether VLMs genuinely comprehend and reason causal relations rather than relying solely on statistical patterns. In this experiment, intervention performance is measured by model selection accuracy. We evaluate 3 popular commercial VLMs on this task: ChatGPT-4o, Gemini-1.5-Pro, and Claude-3.5-Haiku[5].

Results and Analysis. As shown in Tab. 2, our experiments indicate that current VLMs struggle to handle complex rules, e.g. magnetic fields, in causal intervention tasks. We found that the models' inferences are dominated by the prior knowledge embedded in the LLMs, while visual cues—despite containing the ground truth—are largely ignored (see Fig. 8).

Table 2: Causal intervention in VLMs: Evaluation using three real-world rules, with accuracy (%) reported.

Models	Reflection	Lens	Mag. Field
ChatGPT	96.67	100.00	50.00
Gemini	100.00	100.00	0.00
Claude	100.00	96.67	13.33

5 Conclusion

Causal3D is a comprehensive benchmark designed to evaluate causal reasoning in visual AI, including causal tasks of discovery, disentanglement, and intervention. Our dataset integrates structured causal graphs with corresponding 3D visual representations, providing a rigorous assessment framework across diverse physical and hypothetical scenes. Experimental results demonstrate that: 1) the performance of current causal discovery algorithms decreases as the

[5]Model versions are those publicly available as of January 2025.

increasing of the complexity of causal structures; 2) for causal representation learning, the current state-of-arts can not well handle our realistic and diverse 3D scenes; 3) commercial VLMs struggle with causal inference based on visual cues and complex scenarios, particularly in hypothetical settings where prior knowledge is absent. CAUSAL3D serves as a critical step toward bridging the gap between traditional causal research and computer vision, enabling a more comprehensive and fine-grained evaluation of causal inference. We envision CAUSAL3D as a foundation for future research, fostering advancements in causal-aware AI models and driving progress toward more reliable and interpretable machine intelligence.

ETHICS STATEMENT

This research adheres to the ICLR Code of Ethics. The study does not involve human subjects, personally identifiable information, or sensitive data. All datasets used are publicly available, and appropriate steps were taken to ensure compliance with privacy, fairness, and research integrity standards. No conflicts of interest or ethical concerns are anticipated.

REPRODUCIBILITY STATEMENT

We conducted extensive experiments with multiple random seeds to ensure the robustness and reproducibility of our results. Detailed descriptions of model architectures, training procedures, and hyperparameters closely follow those reported in the original baseline papers. The data generation code is submitted in a zip file as supplementary materials.

REFERENCES

SeungHwan An, Kyungwoo Song, and Jong-June Jeon. Causally disentangled generative variational autoencoder. In *ECAI 2023*, pages 93–100. IOS Press, 2023.

Tayfun Ates, M. Ateşoğlu, Çağatay Yiğit, Ilker Kesen, Mert Kobas, Erkut Erdem, Aykut Erdem, Tilbe Goksun, and Deniz Yuret. CRAFT: A benchmark for causal reasoning about forces and inTeractions. In Smaranda Muresan, Preslav Nakov, and Aline Villavicencio, editors, *Findings of the Association for Computational Linguistics: ACL 2022*, pages 2602–2627, Dublin, Ireland, May 2022. Association for Computational Linguistics. doi: 10.18653/v1/2022.findings-acl.205. URL https://aclanthology.org/2022.findings-acl.205/.

Taiyu Ban, Lyvzhou Chen, Xiangyu Wang, and Huanhuan Chen. From query tools to causal architects: Harnessing large language models for advanced causal discovery from data, 2023. URL https://arxiv.org/abs/2306.16902.

Peter Bühlmann, Jonas Peters, and Jan Ernest. Cam: Causal additive models, high-dimensional order search and penalized regression. *The Annals of Statistics*, 42(6), December 2014. ISSN 0090-5364. doi: 10.1214/14-aos1260. URL http://dx.doi.org/10.1214/14-AOS1260.

Maria Victoria Carro, Francisca Gauna Selasco, Denise Alejandra Mester, Margarita Gonzales, Mario A. Leiva, Maria Vanina Martinez, and Gerardo I. Simari. Do large language models show biases in causal learning?, 2024. URL https://arxiv.org/abs/2412.10509.

David Maxwell Chickering. Learning equivalence classes of bayesian-network structures. *The Journal of Machine Learning Research*, 2:445–498, 2002.

Martina Cinquini, Fosca Giannotti, and Riccardo Guidotti. Boosting synthetic data generation with effective nonlinear causal discovery. In *2021 IEEE Third International Conference on Cognitive Machine Intelligence (CogMI)*, pages 54–63. IEEE, 2021.

Zizhen Deng, Xiaolong Zheng, Hu Tian, and Daniel Dajun Zeng. Deep causal learning: representation, discovery and inference. *arXiv preprint arXiv:2211.03374*, 2022.

Alexey Dosovitskiy, Lucas Beyer, Alexander Kolesnikov, Dirk Weissenborn, Xiaohua Zhai, Thomas Unterthiner, Mostafa Dehghani, Matthias Minderer, Georg Heigold, Sylvain Gelly, Jakob Uszkoreit, and Neil Houlsby. An image is worth 16x16 words: Transformers for image recognition at scale. In *International Conference on Learning Representations (ICLR)*, 2021. URL https://openreview.net/forum?id=YicbFdNTTy.

Yuxin Fang, Wen Wang, Binhui Xie, Quan Sun, Ledell Wu, Xinggang Wang, Tiejun Huang, Xinlong Wang, and Yue Cao. EVA: Exploring the limits of masked visual representation learning at scale. In *Proceedings of the IEEE/CVF Conference on Computer Vision and Pattern Recognition*, pages 19358–19369, 2023.

Zhijing Jin, Yuen Chen, Felix Leeb, Luigi Gresele, Ojasv Kamal, Zhiheng Lyu, Kevin Blin, Fernando Gonzalez Adauto, Max Kleiman-Weiner, Mrinmaya Sachan, et al. Cladder: A benchmark to assess causal reasoning capabilities of language models. *Advances in Neural Information Processing Systems*, 36, 2024.

Thomas Jiralerspong, Xiaoyin Chen, Yash More, Vedant Shah, and Yoshua Bengio. Efficient causal graph discovery using large language models, 2024. URL https://arxiv.org/abs/2402.01207.

Emre Kıcıman, Robert Ness, Amit Sharma, and Chenhao Tan. Causal reasoning and large language models: Opening a new frontier for causality. *arXiv preprint arXiv:2305.00050*, 2023.

Aneesh Komanduri, Yongkai Wu, Feng Chen, and Xintao Wu. Learning causally disentangled representations via the principle of independent causal mechanisms. *arXiv preprint arXiv:2306.01213*, 2023.

Sébastien Lachapelle, Philippe Brouillard, Tristan Deleu, and Simon Lacoste-Julien. Gradient-based neural dag learning, 2020. URL https://arxiv.org/abs/1906.02226.

Xiaoyu Liu, Paiheng Xu, Junda Wu, Jiaxin Yuan, Yifan Yang, Yuhang Zhou, Fuxiao Liu, Tianrui Guan, Haoliang Wang, Tong Yu, Julian McAuley, Wei Ai, and Furong Huang. Large language models and causal inference in collaboration: A comprehensive survey, 2024a. URL https://arxiv.org/abs/2403.09606.

Xiaoyu Liu, Paiheng Xu, Junda Wu, Jiaxin Yuan, Yifan Yang, Yuhang Zhou, Fuxiao Liu, Tianrui Guan, Haoliang Wang, Tong Yu, et al. Large language models and causal inference in collaboration: A comprehensive survey. *arXiv preprint arXiv:2403.09606*, 2024b.

Yang Liu, Yu-Shen Wei, Hong Yan, Guan-Bin Li, and Liang Lin. Causal reasoning meets visual representation learning: A prospective study. *Machine Intelligence Research*, 19(6):485–511, 2022.

Ze Liu, Yutong Lin, Yue Cao, Han Hu, Yixuan Wei, Zheng Zhang, Stephen Lin, and Baining Guo. Swin transformer: Hierarchical vision transformer using shifted windows. In *Proceedings of the IEEE/CVF International Conference on Computer Vision (ICCV)*, pages 10012–10022, 2021. doi: 10.1109/ICCV48922.2021.00986.

Ziwei Liu, Ping Luo, Xiaogang Wang, and Xiaoou Tang. Deep learning face attributes in the wild. In *Proceedings of the IEEE International Conference on Computer Vision (ICCV)*, pages 3730–3738, 2015. doi: 10.1109/ICCV.2015.425. URL http://mmlab.ie.cuhk.edu.hk/projects/CelebA.html.

Jing Ma. Causal inference with large language model: A survey. *arXiv preprint arXiv:2409.09822*, 2024.

J. Mao, X. Yang, X. Zhang, N. Goodman, and J. Wu. Clevrer-humans: Describing physical and causal events the human way. In *Advances in Neural Information Processing Systems*, volume 35, pages 7755–7768, 2022.

Judea Pearl. *Causality*. Cambridge university press, 2009.

Atul Rawal, Adrienne Raglin, Qianlong Wang, and Ziying Tang. Investigating causal reasoning in large language models. In *Causality and Large Models @NeurIPS 2024*, 2024. URL https://openreview.net/forum?id=EGWrfirmIM.

Paul Rolland, Volkan Cevher, Matthäus Kleindessner, Chris Russell, Dominik Janzing, Bernhard Schölkopf, and Francesco Locatello. Score matching enables causal discovery of nonlinear additive noise models. In *International Conference on Machine Learning*, pages 18741–18753. PMLR, 2022.

Jakob Runge. Causal network reconstruction from time series: From theoretical assumptions to practical estimation. *Chaos: An Interdisciplinary Journal of Nonlinear Science*, 28(7):075310, 2018. doi: 10.1063/1.5025050. URL https://doi.org/10.1063/1.5025050.

Jakob Runge, Sebastian Bathiany, Erik Bollt, Gustau Camps-Valls, Dim Coumou, Ethan Deyle, Clark Glymour, Marlene Kretschmer, Miguel D Mahecha, Jordi Muñoz-Marí, et al. Inferring causation from time series in earth system sciences. *Nature communications*, 10(1):1–13, 2019a.

Jakob Runge, Peer Nowack, Marlene Kretschmer, Seth Flaxman, and Dino Sejdinovic. Detecting and quantifying causal associations in large nonlinear time series datasets. *Science Advances*, 5 (11):eaau4996, 2019b. doi: 10.1126/sciadv.aau4996. URL https://www.science.org/doi/10.1126/sciadv.aau4996.

Fabrizio Russo and Francesca Toni. Causal discovery and knowledge injection for contestable neural networks (with appendices), 2023. URL https://arxiv.org/abs/2205.09787.

Pedro Sanchez, Xiao Liu, Alison Q O'Neil, and Sotirios A. Tsaftaris. Diffusion models for causal discovery via topological ordering, 2023. URL https://arxiv.org/abs/2210.06201.

Bernhard Schölkopf. Causality for machine learning. In *Probabilistic and causal inference: The works of Judea Pearl*, pages 765–804. 2022.

Bernhard Schölkopf, Francesco Locatello, Stefan Bauer, Nan Rosemary Ke, Nal Kalchbrenner, Anirudh Goyal, and Yoshua Bengio. Toward causal representation learning. *Proceedings of the IEEE*, 109(5):612–634, 2021.

ChengAo Shen, Zhengzhang Chen, Dongsheng Luo, Dongkuan Xu, Haifeng Chen, and Jingchao Ni. Exploring multi-modal integration with tool-augmented llm agents for precise causal discovery. *arXiv preprint arXiv:2412.13667*, 2024.

Xinwei Shen, Furui Liu, Hanze Dong, Qing Lian, Zhitang Chen, and Tong Zhang. Weakly supervised disentangled generative causal representation learning, 2022. URL https://arxiv.org/abs/2010.02637.

Mannat Singh, Laura Gustafson, Aaron Adcock, Vinicius de Freitas Reis, Bugra Gedik, Raj Prateek Kosaraju, Dhruv Mahajan, Ross Girshick, Piotr Dollár, and Laurens van der Maaten. Revisiting weakly supervised pre-training of visual perception models. In *Proceedings of the IEEE/CVF Conference on Computer Vision and Pattern Recognition*, pages 804–814, 2022.

Peter Spirtes, Clark Glymour, and Richard Scheines. *Causation, Prediction, and Search*. MIT Press, 2nd edition, 2000a. ISBN 978-0262194402.

Peter Spirtes, Clark N Glymour, and Richard Scheines. *Causation, prediction, and search*. MIT press, 2000b.

Ruibo Tu, Zineb Senane, Lele Cao, Cheng Zhang, Hedvig Kjellström, and Gustav Eje Henter. Causality for tabular data synthesis: A high-order structure causal benchmark framework, 2024. URL https://arxiv.org/abs/2406.08311.

H. Y. Tung, M. Ding, Z. Chen, D. Bear, C. Gan, J. Tenenbaum, and K. Smith. Physion++: Evaluating physical scene understanding that requires online inference of different physical properties. In *Advances in Neural Information Processing Systems*, volume 36, 2024.

J. Von Kügelgen, Y. Sharma, L. Gresele, W. Brendel, B. Schölkopf, M. Besserve, and F. Locatello. Self-supervised learning with data augmentations provably isolates content from style. In *Advances in Neural Information Processing Systems*, volume 34, pages 16451–16467, 2021.

Guangya Wan, Yuqi Wu, Mengxuan Hu, Zhixuan Chu, and Sheng Li. Bridging causal discovery and large language models: A comprehensive survey of integrative approaches and future directions, 2024. URL https://arxiv.org/abs/2402.11068.

Liuyi Wang, Zongtao He, Ronghao Dang, Mengjiao Shen, Chengju Liu, and Qijun Chen. Vision-and-language navigation via causal learning. In *Proceedings of the IEEE/CVF Conference on Computer Vision and Pattern Recognition*, pages 13139–13150, 2024a.

Wenhai Wang, Jifeng Dai, Zhe Chen, Zhenhang Huang, Zhiqi Li, Xizhou Zhu, Xiaowei Hu, Tong Lu, Lewei Lu, Hongsheng Li, Xiaogang Wang, and Yu Qiao. Internimage: Exploring large-scale vision foundation models with deformable convolutions. In *Proceedings of the IEEE/CVF Conference on Computer Vision and Pattern Recognition*, pages 14408–14419, 2023. doi: 10.1109/CVPR52729.2023.01440.

Xinyue Wang, Kun Zhou, Wenyi Wu, Fang Nan, and Biwei Huang. Causal-copilot: An autonomous causal analysis agent. 2024b.

Bingyang Wen, Luis Oliveros Colon, K. P. Subbalakshmi, and R. Chandramouli. Causal-tgan: Generating tabular data using causal generative adversarial networks, 2021. URL https://arxiv.org/abs/2104.10680.

Bingyang Wen, Yupeng Cao, Fan Yang, Koduvayur Subbalakshmi, and Rajarathnam Chandramouli. Causal-tgan: Modeling tabular data using causally-aware gan. In *ICLR Workshop on Deep Generative Models for Highly Structured Data*, 2022.

Anpeng Wu, Kun Kuang, Minqin Zhu, Yingrong Wang, Yujia Zheng, Kairong Han, Baohong Li, Guangyi Chen, Fei Wu, and Kun Zhang. Causality for large language models, 2024. URL https://arxiv.org/abs/2410.15319.

Mengyue Yang, Furui Liu, Zhitang Chen, Xinwei Shen, Jianye Hao, and Jun Wang. Causalvae: Structured causal disentanglement in variational autoencoder, 2023. URL https://arxiv.org/abs/2004.08697.

Muyu Yang, Feng Liu, Zhi Chen, Xi Shen, Jie Hao, and Jianmin Wang. Causalvae: Structured causal disentanglement in variational autoencoder. *arXiv preprint arXiv:2004.08697*, 2020. URL https://arxiv.org/abs/2004.08697.

Tian-Le Yang, Kuang-Yao Lee, Kun Zhang, and Joe Suzuki. Functional linear non-gaussian acyclic model for causal discovery, 2024. URL https://arxiv.org/abs/2401.09641.

Xu Yang, Hanwang Zhang, Guojun Qi, and Jianfei Cai. Causal attention for vision-language tasks. In *Proceedings of the IEEE/CVF conference on computer vision and pattern recognition*, pages 9847–9857, 2021.

Zhuolin Yang, Zhikuan Zhao, Boxin Wang, Jiawei Zhang, Linyi Li, Hengzhi Pei, Bojan Karlaš, Ji Liu, Heng Guo, Ce Zhang, et al. Improving certified robustness via statistical learning with logical reasoning. *Advances in Neural Information Processing Systems*, 35:34859–34873, 2022.

Yue Yu, Jie Chen, Tian Gao, and Mo Yu. Dag-gnn: Dag structure learning with graph neural networks, 2019. URL https://arxiv.org/abs/1904.10098.

Shitian Zhao, Zhuowan Li, Yadong Lu, Alan Yuille, and Yan Wang. Causal-cog: A causal-effect look at context generation for boosting multi-modal language models. In *Proceedings of the IEEE/CVF Conference on Computer Vision and Pattern Recognition*, pages 13342–13351, 2024.

Xun Zheng, Bryon Aragam, Pradeep Ravikumar, and Eric P. Xing. Dags with no tears: Continuous optimization for structure learning. In *Advances in Neural Information Processing Systems*, volume 31, pages 9472–9483, 2018. URL https://papers.nips.cc/paper/2018/hash/e347c51419ffb23ca3fd5050202f9c3d-Abstract.html.

Robin S Zimmermann, Yash Sharma, Steffen Schneider, Matthias Bethge, and Wieland Brendel. Contrastive learning inverts the data generating process. In *Proceedings of the International Conference on Machine Learning (ICML)*, pages 12979–12990. PMLR, July 2021.

APPENDIX

In the appendix, we will supplement the scenes and their data details that were not presented in the main text. Additionally, we will also display the remaining experiment setups and results.

6 ADDITIONAL SCENES AND DATA DETAILS

Fig. 9, Fig. 10, and Fig. 11 show the dataset details of different scenes, including the following information: name of scenes, the number of causal variables (i.e., nodes in causal graph), the relation types (linear or non-linear), causal graphs, and structural equations. For realistic scenes, we also add a brief description. Furthermore, we showcase all the scenes by randomly sampling 2D images from different viewpoints and surroundings for illustration (shown from Fig. 12 to Fig. 36). For notational simplicity, we omit the exogenous noise variables in the structural equations, all of which follow uniform distributions. For example, in the Reflection scene, the expression $A = B$ is a shorthand for the structural equation $B = A + \epsilon$, where ϵ is an independent uniform noise term. This non-Gaussianity ensures the identifiability of the causal direction $A \to B$.

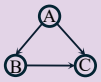
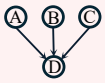
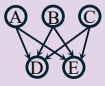
Scene	Description	Causal Graph		Structure Equation
Reflection, Linear	*Light reflects off a mirror.*		A: Incident light. B: Outgoing light.	$A = B$
Seesaw, Non-Linear	*A seesaw with a cylinder on each end.*		A: Left torque. B: Right torque. C: Seesaw tilt direction.	$C = sign(A - B)$
Convex Lens, Non-Linear	*A candle and its image formed by a convex lens.*		A: Distance from lens to the object. B: Distance from the lens to the image. C: Magnification factor.	$\frac{1}{f} = \frac{1}{A} + \frac{1}{B}$ f is the focal length, which is a constant. $C = -\frac{A}{B}$
Magnet, Non-Linear	*A magnet and a needle displaying its magnetic field.*		A: Rotation angle of the bar magnet. B: The x-coordinate of the magnetic needle. C: The y-coordinate of the magnetic needle. D: Orientation of the magnetic field at the needle.	$D = \frac{\mu_0}{4\pi}\left(\frac{3\overrightarrow{(B,C)}\vec{A}\overrightarrow{(B,C)}}{\overrightarrow{(B,C)}^5} - \frac{\vec{A}}{\overrightarrow{(B,C)}^3}\right)$
Pendulum, Non-Linear	*A light source, a pendulum, and its shadow.*		A: Light position. B: Pendulum angle. C: Pendulum length. D: Shadow middle point position. E: Shadow length.	$D = \frac{1}{2}\left(-\frac{y_l x_p + y_l CsinB + ACcosB - y_p A}{y_p - CcosB - y_l} - \frac{y_l x_p - y_p A}{y_p - y_l}\right)$ $E = -\frac{y_l x_p + y_l CsinB + ACcosB - y_p A}{y_p - CcosB - y_l} + -\frac{y_l x_p + y_l CsinB + ACcosB - y_p A}{y_p - CcosB - y_l}$ (x_p, y_p) is the coordinate of the pendulum end point. y_l is the y-coordinate of the light.

Figure 9: Data details of realistic scenes (as a supplement to Fig. 1).

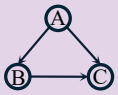
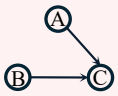
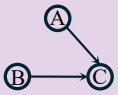
Scene	Causal Graph		Structure Equation
2 Variables, Linear		A: Volume of the ball. B: Volume of the cube.	$B = 1.5A$
2 Variables, Non-Linear		A: Volume of the ball. B: Volume of the cube.	$B = \cos(A)$
3 Variables, Fully Connected, Linear		A: Volume of the ball. B: Height of the cuboid. C: Base area of the cone.	$B = 4A$ $C = -10A + 10B$
3 Variables, V-Structure, Linear		A: Volume of the ball. B: Height of the cuboid. C: Base area of the cone.	$C = 0.4A + 0.7B$
3 Variables, V-Structure, Non-Linear		A: Volume of the ball. B: Height of the cuboid. C: Base area of the cone.	$C = \tan(A) + 0.7B$

Figure 10: Data details of hypothetical scenes (2 variables and 3 variables).

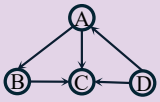
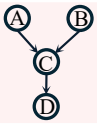
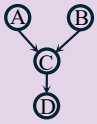
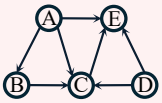
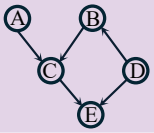
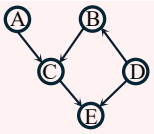
Scene	Causal Graph	Structure Equation
4 Variables, No V-structure Linear	 A: Volume of the ball. B: Volume of the cube. C: Base area of the cuboid. D: Base area of the cone.	$A = 0.5D$ $B = 0.3A$ $C = 0.4A + 0.6B + 0.9B$
4 Variables, V-Structure, Linear	 A: Volume of the ball. B: Volume of the cube. C: Base area of the cuboid. D: Base area of the cone.	$C = 0.3A + 0.7B$ $D = 0.4C$
4 Variables, V-Structure, Non-Linear	 A: Volume of the ball. B: Volume of the cube. C: Base area of the cuboid. D: Base area of the cone.	$C = 50\sin(A) + 20B$ $D = 1100\cos(C)$
5 Variables, No V-structure Linear	 A: Volume of the ball. B: Volume of the cube. C: Base area of the cuboid. D: Base area of the cone. E: Height of the cone.	$B = 0.01A$ $C = -0.01A + 16B$ $D = 1.2C$ $E = 5A - 0.5C + 2D$
5 Variables, V-Structure, Linear	 A: Volume of the ball. B: Volume of the cube. C: Base area of the cuboid. D: Base area of the cone. E: Height of the cone.	$B = 0.045D$ $C = 0.03A + 10B$ $E = 0.01C + 0.02D$
5 Variables, V-Structure, Non-Linear	 A: Volume of the ball. B: Volume of the cube. C: Base area of the cuboid. D: Base area of the cone. E: Height of the cone.	$B = 60\sin(D)$ $C = 400\cos(A) + 20B$ $E = 35\tan(C) + 0.1D$

Figure 11: Data details of hypothetical scenes (4 variables and 5 variables).

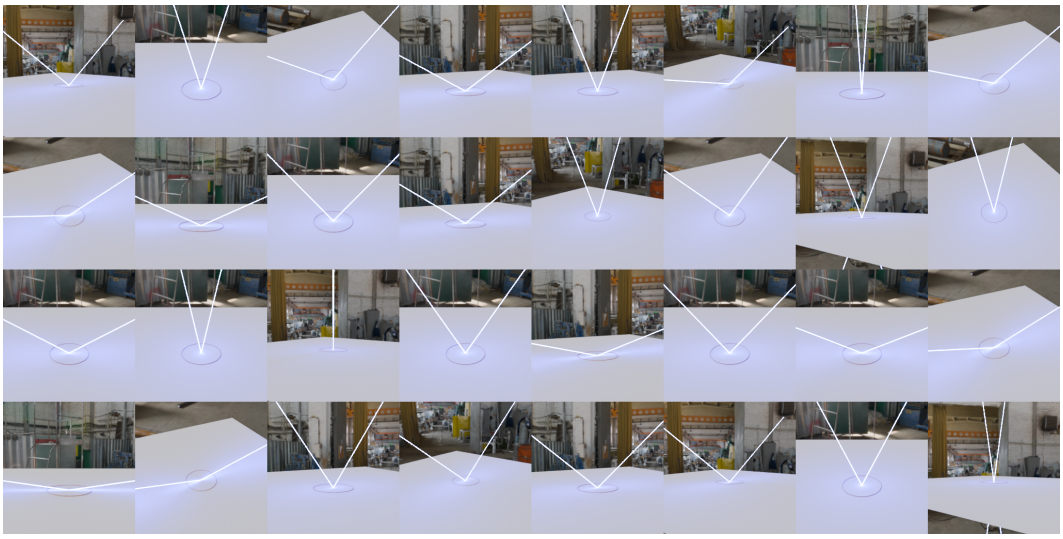


Figure 12: Reflection (Real Background).

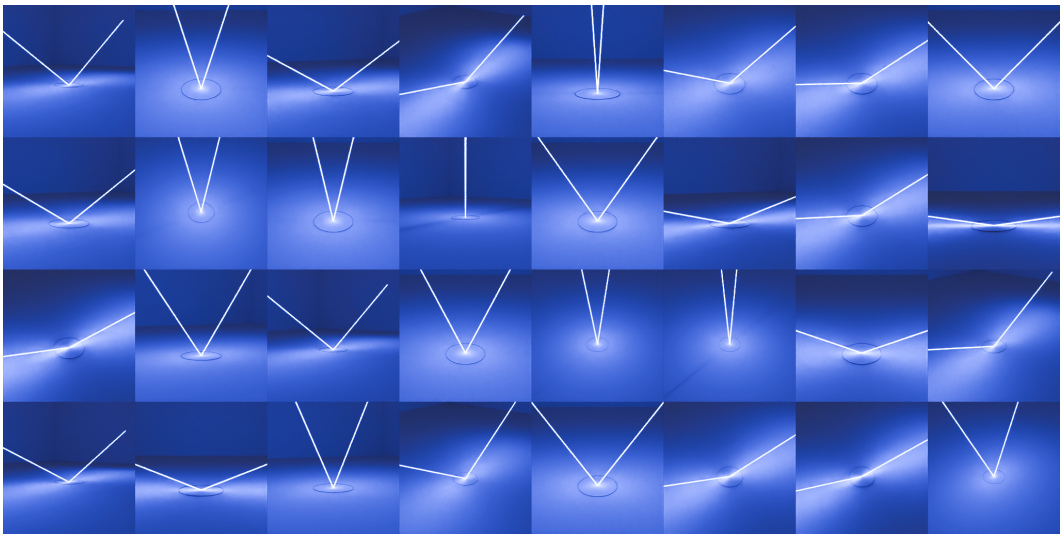


Figure 13: Reflection (Virtual Background).

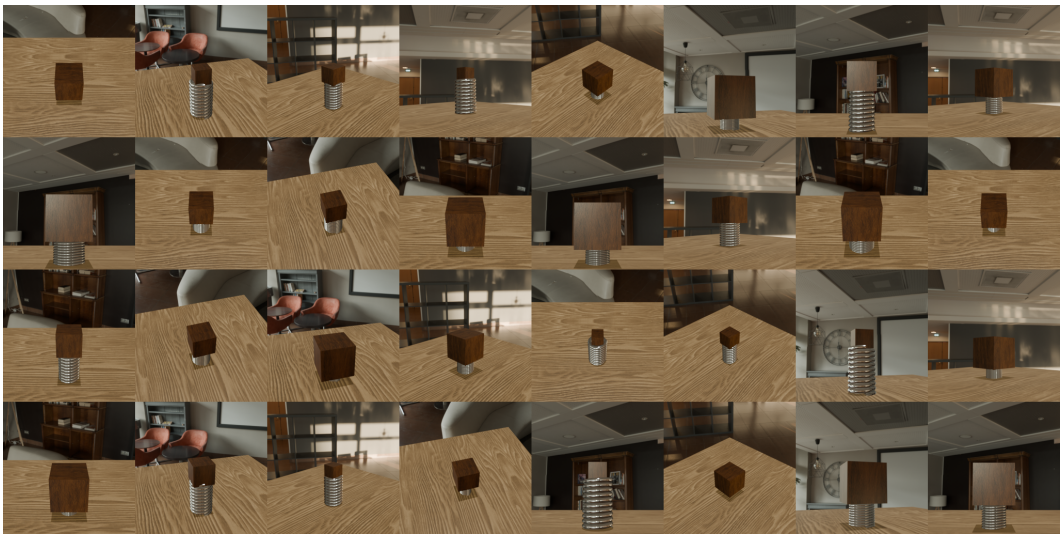


Figure 14: Spring (Real Background).

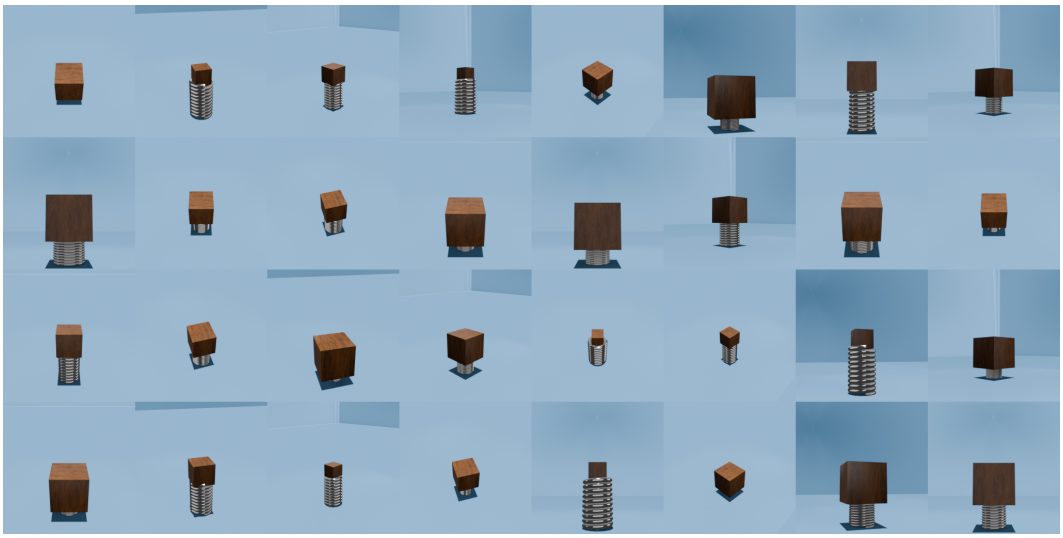


Figure 15: Spring (Virtual Background).

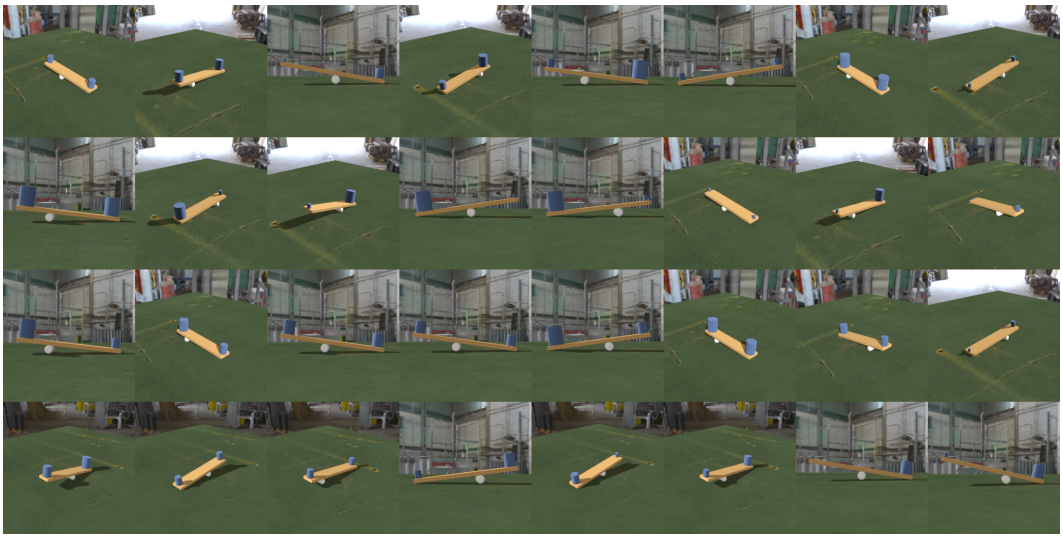


Figure 16: Seesaw (Real Background).

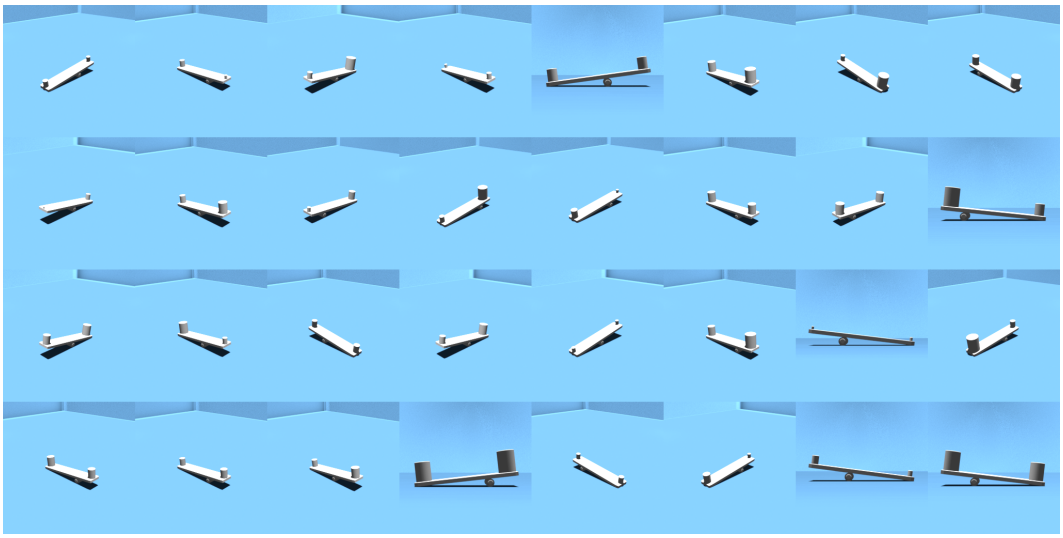


Figure 17: Seesaw (Virtual Background).

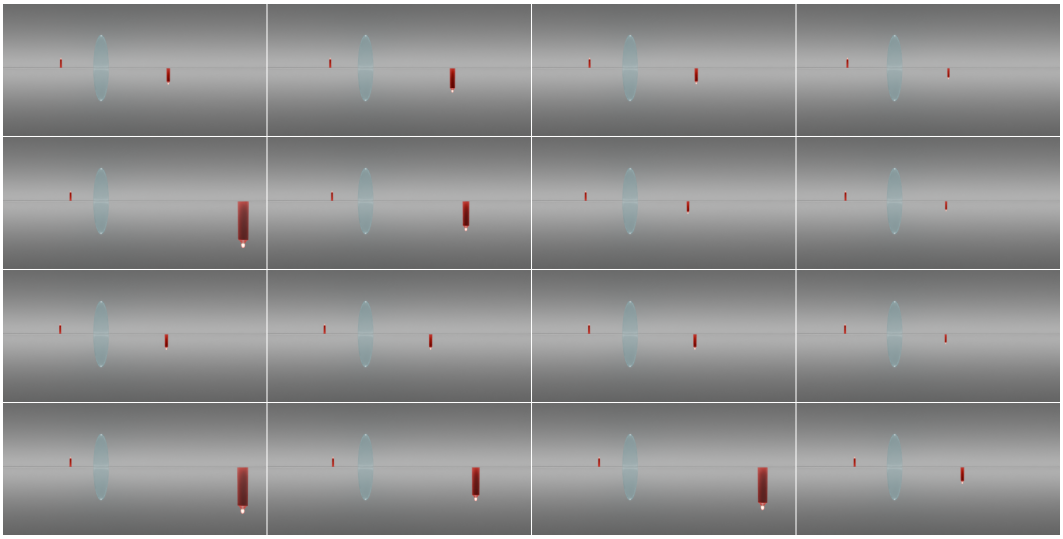


Figure 18: Convex Lens.

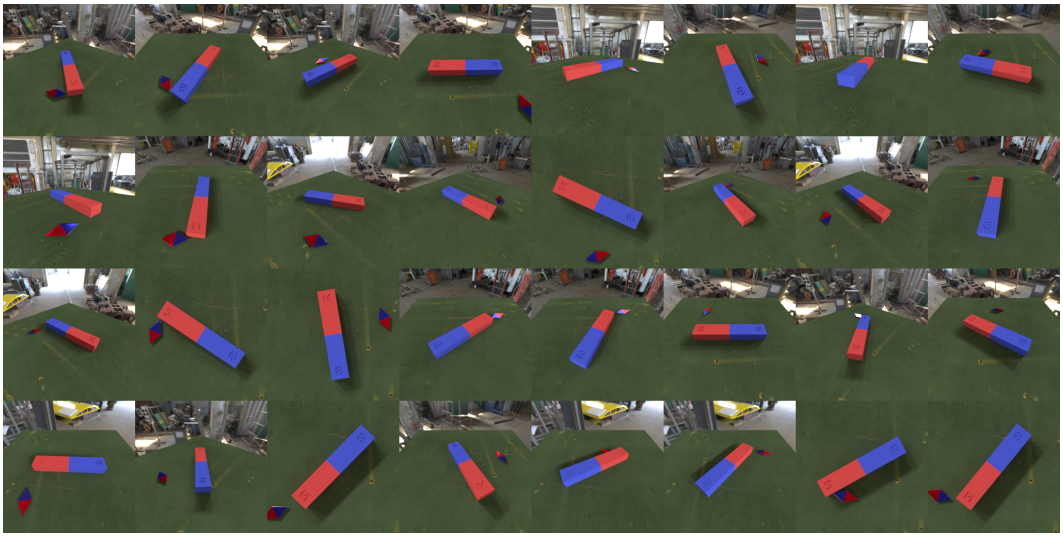


Figure 19: Magnet (Real Background).

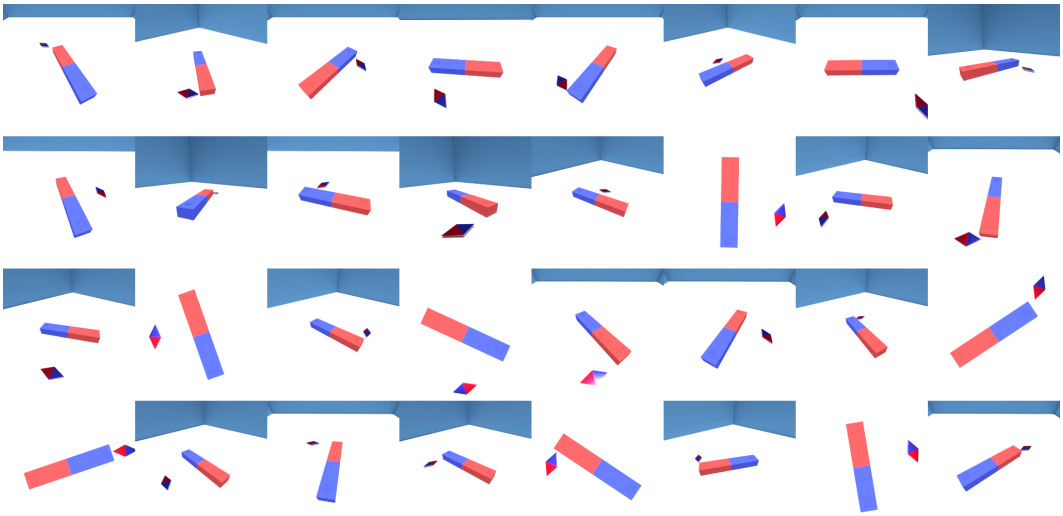


Figure 20: Magnet (Virtual Background).

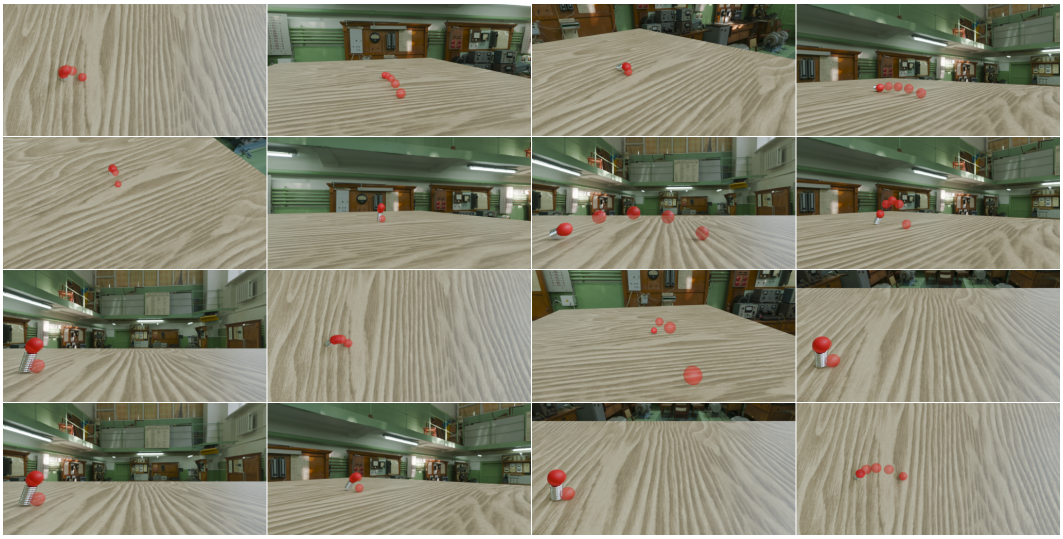


Figure 21: Parabola (Real Background).

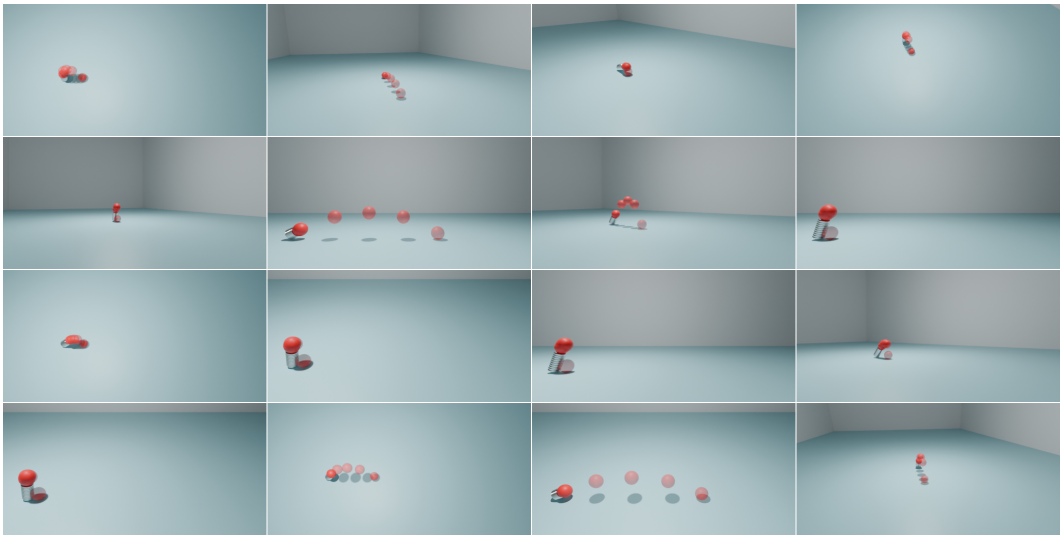


Figure 22: Parabola (Virtual Background).

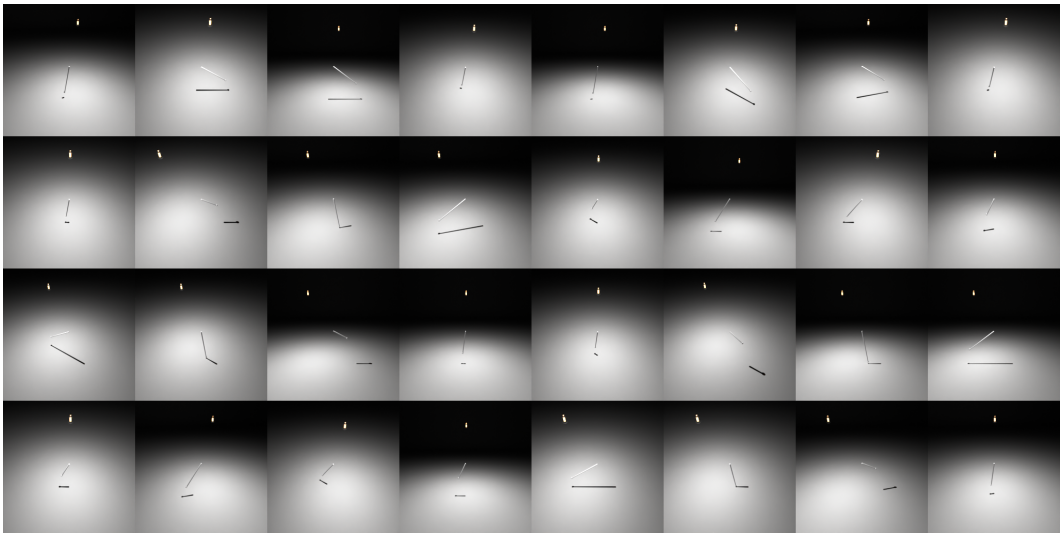


Figure 23: Pendulum.



Figure 24: Water Flow (Real Background).

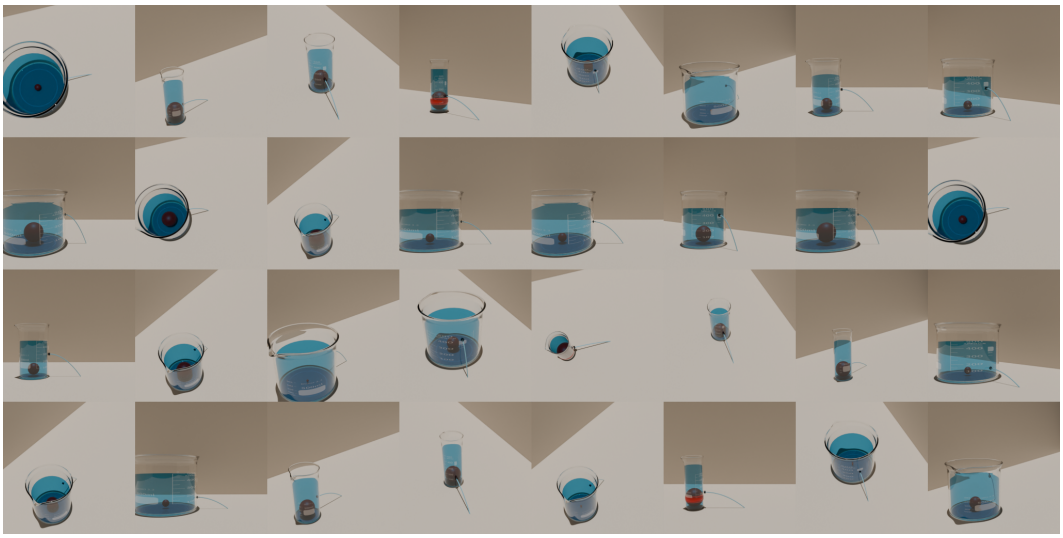


Figure 25: Water Flow (Virtual Background).

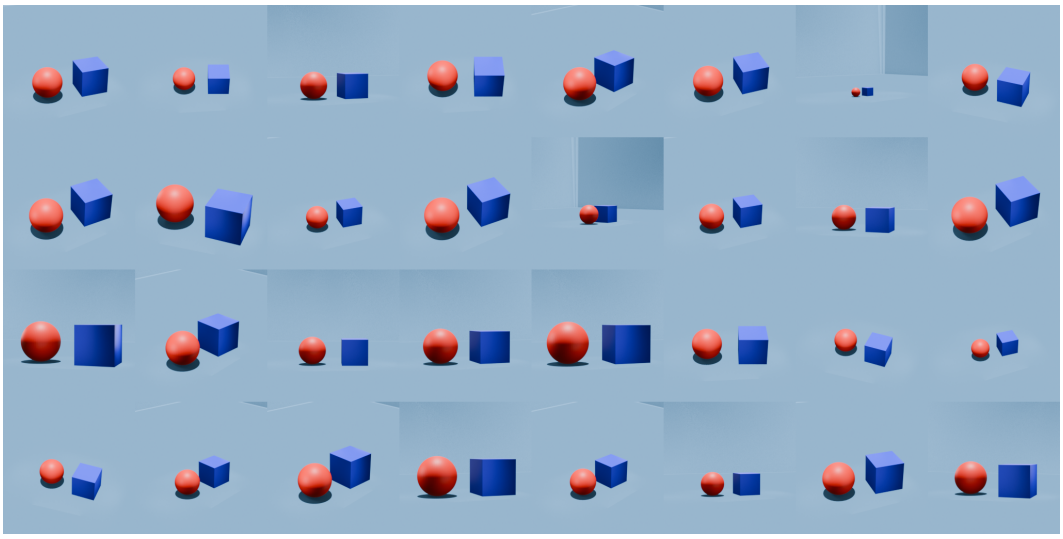


Figure 26: Hypothetical Scene (2 Variables, Linear).

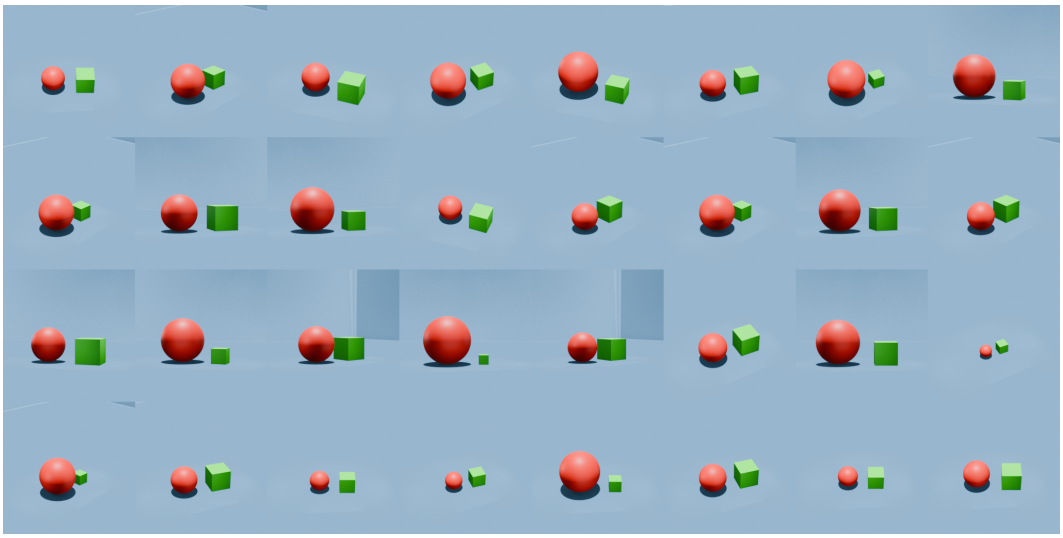


Figure 27: Hypothetical Scene (2 Variables, Non-Linear).

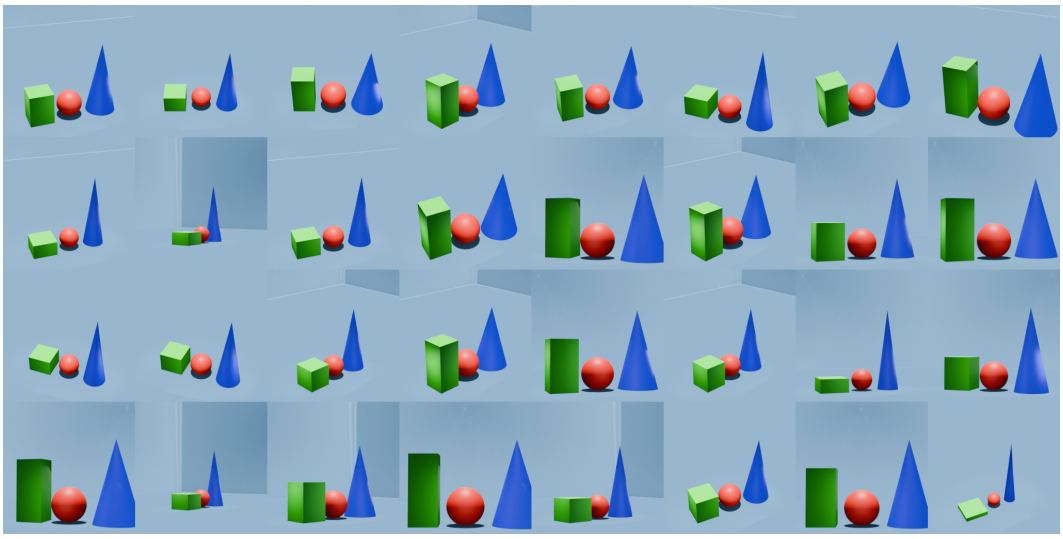


Figure 28: Hypothetical Scene (3 Variables, Linear, Fully-Connected).

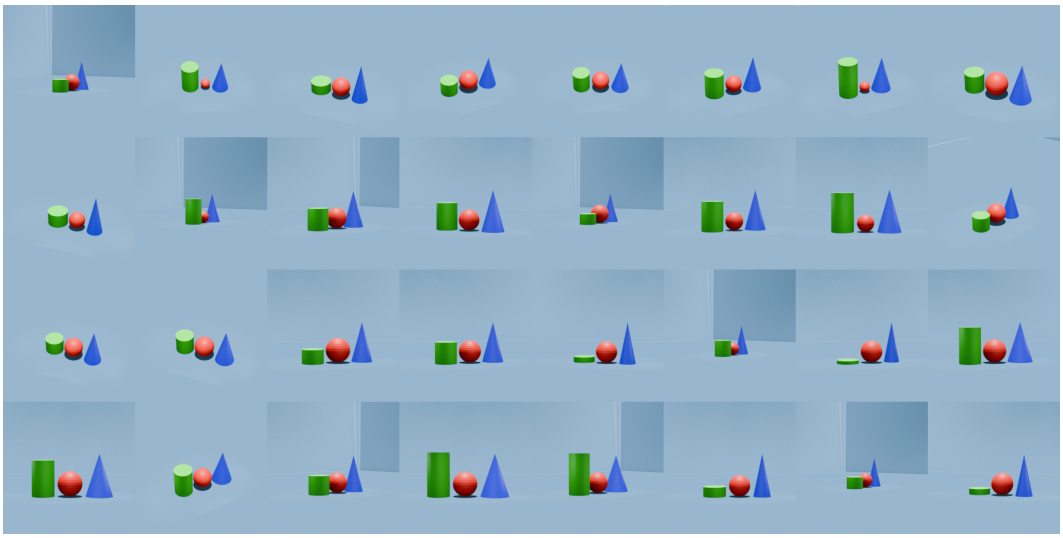


Figure 29: Hypothetical Scene (3 Variables, Linear, V-Structure).

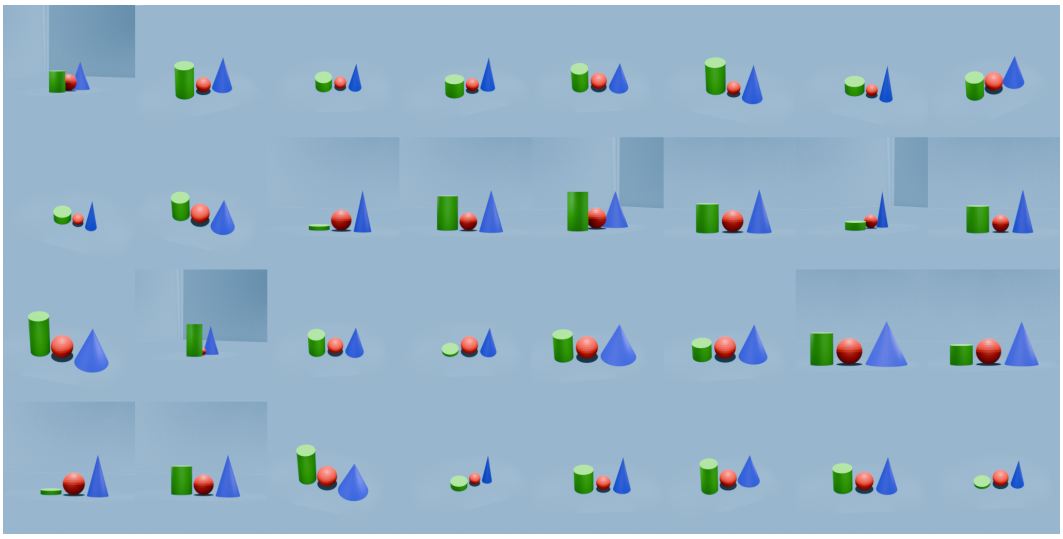


Figure 30: Hypothetical Scene (3 Variables, Non-Linear, V-Structure).

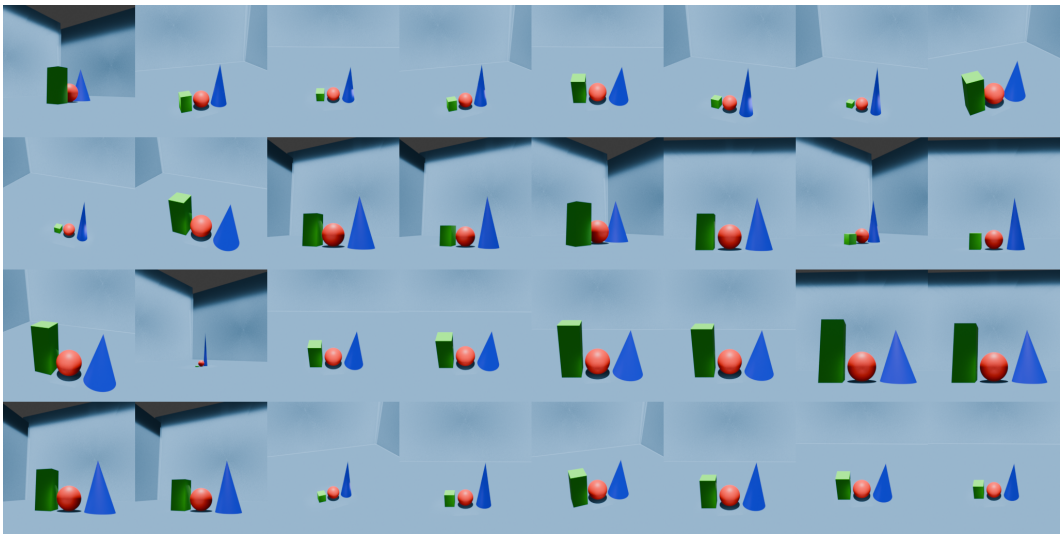


Figure 31: Hypothetical Scene (4 Variables, Linear, Fully-Connected).

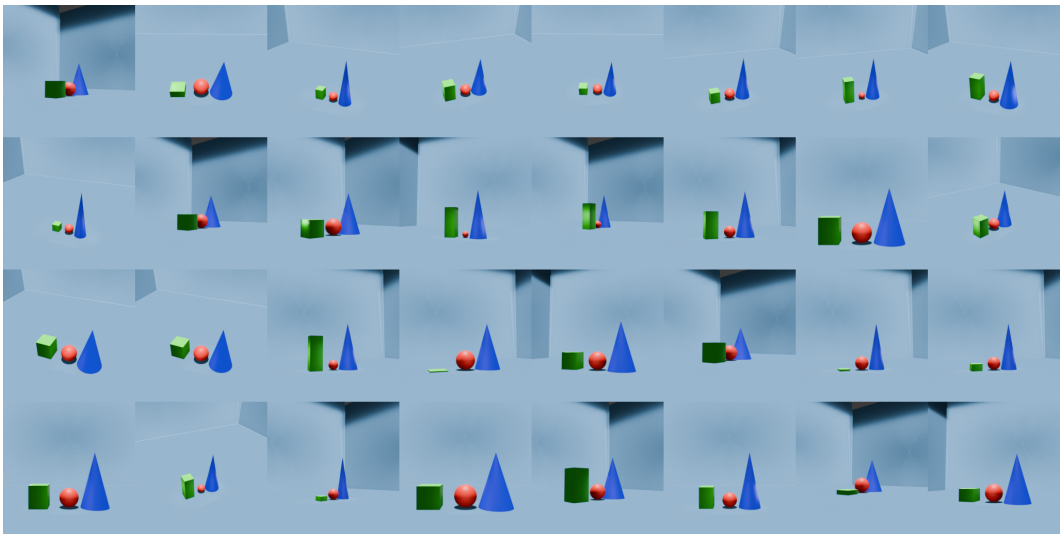


Figure 32: Hypothetical Scene (4 Variables, Linear, V-Structure).

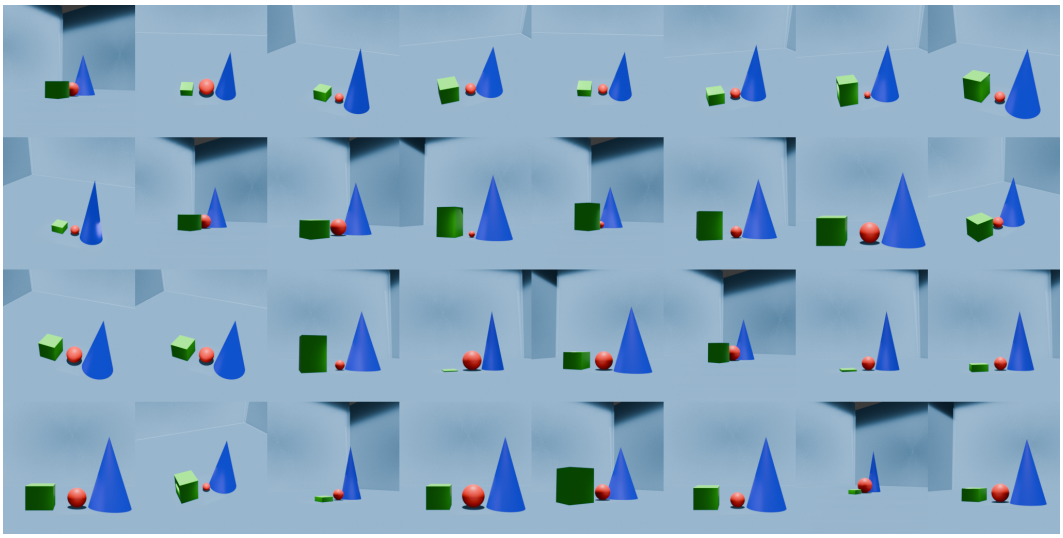


Figure 33: Hypothetical Scene (4 Variables, Non-Linear, V-Structure).

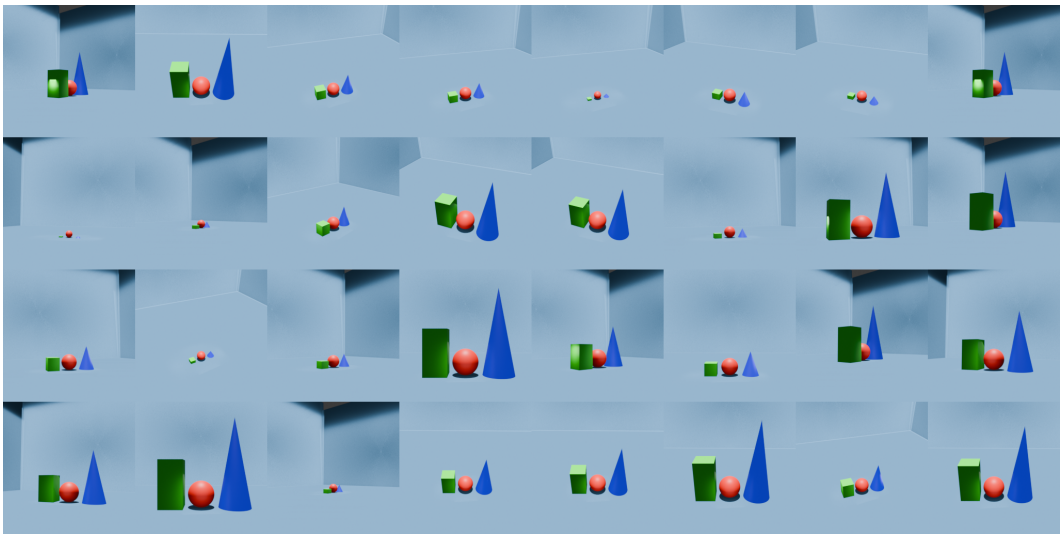


Figure 34: Hypothetical Scene (5 Variables, Linear, Fully-Connected).

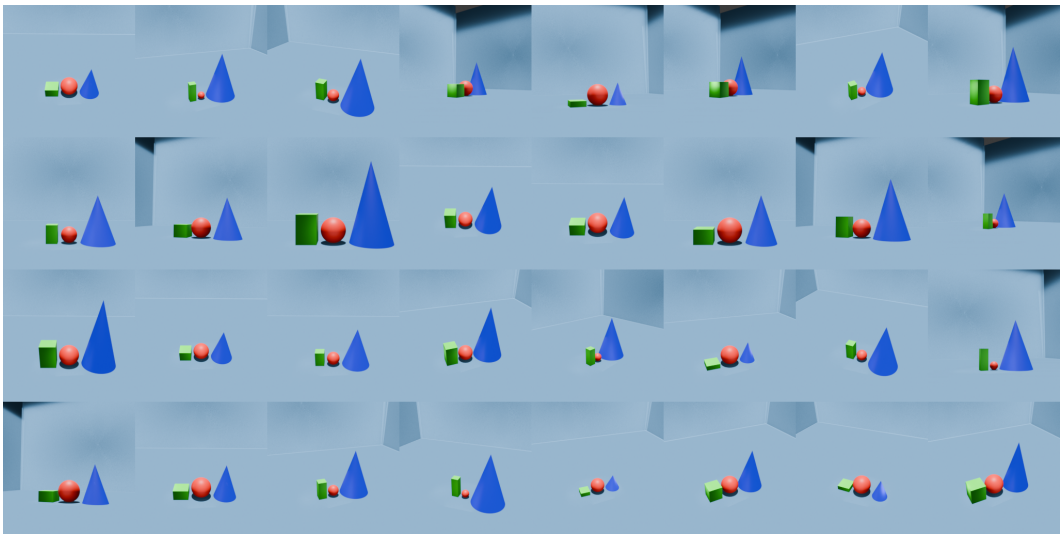


Figure 35: Hypothetical Scene (5 Variables, Linear, V-Structure).

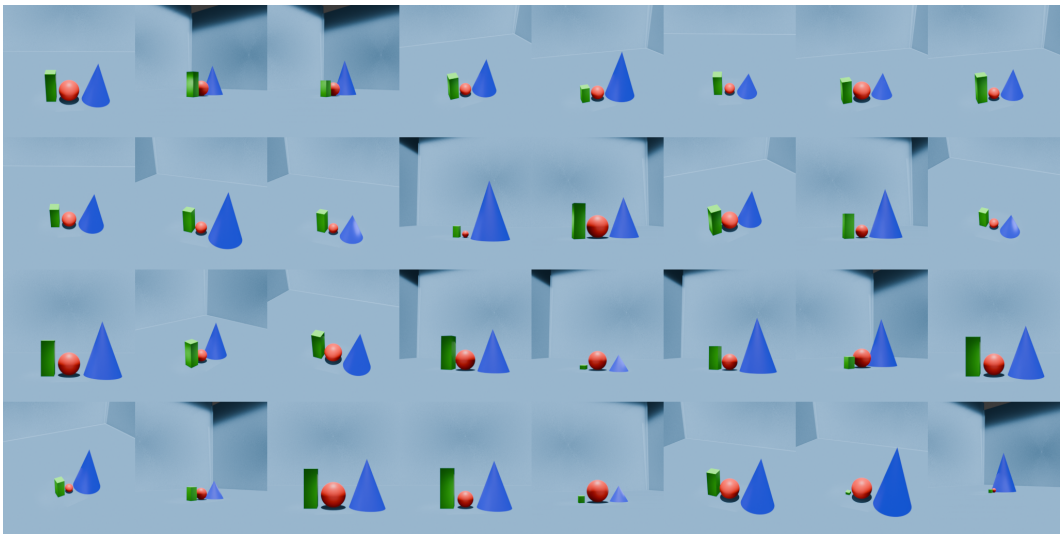


Figure 36: Hypothetical Scene (5 Variables, Non-Linear, V-Structure).

7 Experiment Details

In this section, we present four detailed prompt strategies for performing causal discovery tasks on VLMs (see Tab. 3). Additionally, the results of causal discovery in 3D scenes through VLMs are also shown in Fig. 37.

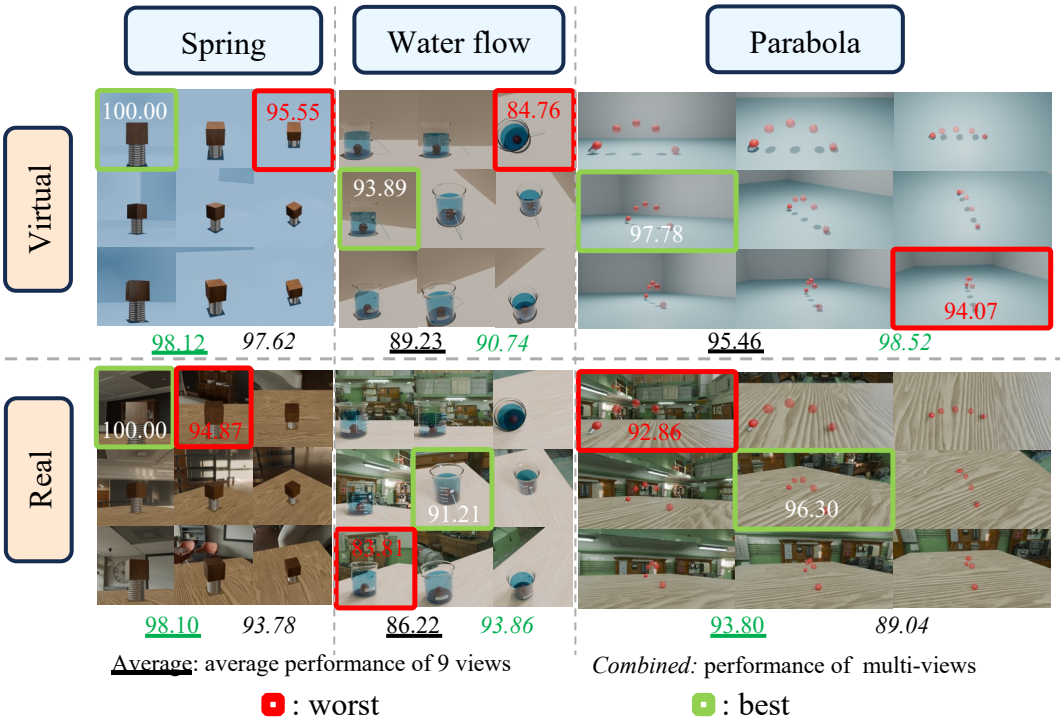


Figure 37: Performance Comparison in 3D scenes: selecting 3 scenes for case studies: Spring, Water flow, and Parabola. Using F1 score as the evaluation metric, we assess inference performance in the causal discovery task. The best and worst views are highlighted to demonstrate the impact of different perspectives. To analyze the effect of multi-view vs. single-view inputs, we average the performance across 9 individual views and compare it with the overall multi-view performance, highlighting the better results in green.

8 Broader Impact

CAUSAL3D advances the integration of causal reasoning in computer vision, contributing to more robust, interpretable, and generalizable AI systems. By introducing a structured benchmark and systematically evaluating state-of-the-art methods, our research provides valuable insights into the challenges and opportunities of causal learning in visual data. The proposed benchmark fosters interdisciplinary collaboration, bridging causal inference, computer vision, and machine learning communities. It serves as a foundation for future research, enabling the development of models that can better generalize across domains, adapt to distribution shifts, and provide meaningful explanations. Furthermore, by improving causal understanding in vision tasks, this work has potential applications in fields such as healthcare, autonomous systems, and scientific discovery, where reliability and transparency are essential. While our evaluation framework is based on the authors' consensus, we encourage community discussions to refine causal reasoning criteria and enhance benchmarking standards. We will release evaluation scripts to support innovation and aid the development of new methodologies. Additionally, we emphasize the responsible use of CAUSAL3D and strictly prohibit any form of data leakage or test set optimization to maintain fairness and integrity in evaluation. Our work does not raise any ethical concerns that require disclosure.

9 LIMITATIONS

Although CAUSAL3D is comprehensive, there remains room for improvement. First, the current benchmark is constructed solely from observational data; incorporating interventional data in the future would enable user interaction and support more interactive causal evaluation. Second, the dataset complexity could be further enriched by introducing more nodes in the causal graphs and incorporating finer-grained visual details, such as textures of objects.

10 THE USE OF LARGE LANGUAGE MODELS (LLMS)

We used ChatGPT, Claude and Gemini to evaluate our datasets. The LLM was not involved in data generation, model training, or writing of technical content.

Table 3: Examples of the four prompt strategies used for causal discovery tasks in VLMs evaluation.

PROMPT STRATEGY	TEMPLATE EXAMPLE
BASIC	**ANALYZE THE PROVIDED IMAGES AND IDENTIFY CAUSAL RELATIONSHIPS BETWEEN THE VARIABLES**. COMPLETE THE CAUSALITY ADJACENCY MATRIX BASED ON THE IDENTIFIED RELATIONSHIPS AND BRIEFLY EXPLAIN YOUR CONCLUSIONS. THERE ARE {VARIABLES}: X, Y, Z. PLEASE FILL THIS CAUSALITY ADJACENCY MATRIX: $\begin{bmatrix} - & - & - \\ - & - & - \\ - & - & - \end{bmatrix}$ IN THIS MATRIX, `MATRIX[I][J] = 1` MEANS VARIABLE i CAUSES VARIABLE j, WHILE `MATRIX[I][J] = 0` MEANS THERE IS NO DIRECT CAUSAL RELATIONSHIP.
EXPLICIT FUNCTION	**YOU ARE A CAUSAL DISCOVERY EXPERT. YOUR OBJECTIVE IS TO ANALYZE THE PROVIDED IMAGES AND IDENTIFY ANY CAUSAL RELATIONSHIPS BETWEEN THE VARIABLES**. USE THE IDENTIFIED RELATIONSHIPS TO COMPLETE THE CAUSALITY ADJACENCY MATRIX AND PROVIDE A BRIEF EXPLANATION SUPPORTING YOUR CONCLUSIONS.THERE ARE VARIABLES: X, Y, Z ...
ZERO-SHOT-COT	ANALYZE THE PROVIDED IMAGES AND IDENTIFY CAUSAL RELATIONSHIPS BETWEEN THE VARIABLES ... **LET'S THINK STEP BY STEP** ...
FEW-SHOT	ANALYZE THE PROVIDED IMAGES AND IDENTIFY CAUSAL RELATIONSHIPS BETWEEN THE VARIABLES ... **EXAMPLE 1**: TO DETERMINE THE CAUSAL RELATIONSHIPS BETWEEN THE SPRING CONSTANT, WEIGHT, AND DEFORMATION OF THE SPRING, WE CAN USE HOOKE'S LAW, WHICH STATES THAT THE FORCE EXERTED BY A SPRING IS DIRECTLY PROPORTIONAL TO THE DEFORMATION (DISPLACEMENT) OF THE SPRING, GIVEN BY: $$F = k \cdot x$$ WHERE: • F IS THE FORCE APPLIED (RELATED TO WEIGHT), • k IS THE SPRING CONSTANT, • x IS THE DEFORMATION OF THE SPRING. FROM THIS, WE CAN INFER: 1. SPRING CONSTANT k AFFECTS THE DEFORMATION OF THE SPRING (x): IF THE SPRING CONSTANT INCREASES, FOR THE SAME WEIGHT, THE DEFORMATION DECREASES. 2. WEIGHT AFFECTS **DEFORMATION OF THE SPRING** (x): AN INCREASE IN WEIGHT CAUSES MORE DEFORMATION. 3. THE SPRING CONSTANT (k) AND **WEIGHT** DO NOT DIRECTLY AFFECT EACH OTHER. BASED ON THESE RELATIONSHIPS, THE CAUSALITY ADJACENCY MATRIX IS: $$\begin{bmatrix} 0 & 0 & 1 \\ 0 & 0 & 1 \\ 0 & 0 & 0 \end{bmatrix}$$ **EXPLANATION:** • ELEMENT (1,3) IS 1 BECAUSE THE SPRING CONSTANT AFFECTS DEFORMATION. • ELEMENT (2,3) IS 1 BECAUSE THE WEIGHT AFFECTS DEFORMATION. • THE OTHER ENTRIES ARE 0 BECAUSE THERE IS NO DIRECT CAUSAL RELATIONSHIP OTHERWISE. **EXAMPLE 2:** ...; **EXAMPLE 3:** ... ;